

**Republic of Iraq**

**Ministry of Higher Education and Scientific Research**

**University of Babylon**

**College of Engineering**

**Civil Engineering Department**



***Predictive Models for Engineering Properties of  
Geopolymer Concrete Incorporating Mineral  
Admixtures  
A Research***

Submitted to the College of Engineering/University of Babylon in Partial  
Fulfilments of the Requirements for the Degree of Diploma in Civil  
Engineering / Construction Materials Engineering

***By***

***Tamara Sebahi Mohsen Redha***

(B.Sc. in Civil Engineering)

***Supervised By***

***Asst. Prof. Dr. Haider Mohammed Owaid***

**2022 AD**

**1443 AH**

بِسْمِ اللَّهِ الرَّحْمَنِ الرَّحِيمِ

﴿قَالُوا سُبْحَانَكَ لَا عِلْمَ لَنَا إِلَّا مَا عَلَّمْتَنَا إِنَّكَ

أَنْتَ الْعَلِيمُ الْحَكِيمُ﴾

صدق الله العظيم

سورة البقرة

الآية (٣٢)

## Certification of the Examining Committee

*We certify that we have read the thesis entitled (**Predictive Models for Engineering Properties of Geopolymer Concrete Incorporating Mineral Admixtures**) and as an examining committee, examined the student (**Tamara Sebahi Mohsen Redha**) in its content and in what is connected with it, and that in our opinion it is adequate as a thesis for the degree of Diploma of Science in Civil Engineering.*

Signature:

Name:

(Chairman)

Date: / / 2022

Signature:

Name:

(Member)

Date: / / 2022

Signature:

Name: (Member)

Date: / / 2022

Signature:

Name:

(Member)

Date: / / 2022

Signature:

Name: *Asst.Prof. Haider M. Owaid*

(Supervisor and Member)

Date: / / 2022

Signature:

Name: *Asst. Prof. Dr. Thair Jabbar Mizhir Alfatlawi*

(Head of Civil Engineering Department)

Date: / / 2022

Signature:

Name: *Prof. Dr. Hatem Hadi Obaid*

(The Acting Dean of the College of Engineering)

Date: / / 2022

## **Supervisor Certification**

*We certify that this thesis which is entitled (**Predictive Models for Engineering Properties of Geopolymer Concrete Incorporating Mineral Admixtures**) has been prepared by (**Tamara Sebah Mohsen Redha**) under my supervision at College of Engineering, Babylon University, in partial fulfilment of the requirements for the degree of Diploma of Science in Civil Engineering.*

Signature:

Name: **Asst. prof. Dr. Haider Mohammed Owaid**

Date: / / 2022



## **Acknowledgments**

*In the name of **Allah**, the most compassionate, the most merciful. Praise be to **Allah**, and pray and peace be on his prophet Mohammed and his family.*

*First, I like to express my appreciation and deepest gratitude to my supervisor **Asst. Prof. Dr. Haider Mohammed Owaid** for his remarkable suggestions, encouragement and guidance throughout the research. I am really indebted to him.*

*I would like to express my deepest feeling of **My family** for their care, patience and great support during the research period.*

*Thanks to all staff of Civil Engineering Department/College of Engineering / University of Babylon for their appreciable support.*

***Tamara Sebahi Mohsen Redha***

*/ /2022*

## **Dedication**

*The deepest words of gratitude and appreciation are the gratitude and dedication of a great person. If you are where I am today, then that is why it deserves a special mention that it is my father. I will not forget to devote the fruits of this effort to those who filled me with supplication, and what I am today God's response to her prayers for me. She is my mother.*

*Sincerity to my family and friends goes for their love, support, guidance, and endless patience in all my endeavours.*

*Tamara Sebahi Mohsen Redha*

*/ /2022*

## Abstract

A new mathematical model for the prediction of the engineering properties of geopolymer concrete incorporating with mineral admixtures materials was proposed and developed in this study using a linear regression equation an artificial neural network (ANN) and Statistical Package for the Social Sciences (SPSS). Mixing proportional elements such as {cement, fine aggregate, coarse aggregate, water to binder , and mineral admixtures such as (fly ash, silica fume, metakaoline, ground granulated blast-furnace slag, and rice husk ash)} were the variables used in the prediction models. Variability was taken as output parameters of the workability and hardened characteristics of geopolymer concrete. The results obtained using the two methods are then compared and discussed. Models provide a reasonable estimate of geopolymer concrete strength properties comprising mineral admixtures materials and have provided good correlations with the data used in this research, according to the review.

The correlation coefficients for fresh concrete preparing including the predicted (slump results) was 0.8778 using SPSS software. While using ANN software gives 0.92 as a correlation coefficient for slump results.

The correlation coefficients for hardened concrete properties including the predicted compressive strength at 3, 7, 28 and 90 days were 0.94, 0.93, 0.91 and 0.96, respectively. And the correlation coefficient for the prediction of splitting tensile strength at 3, 7, 28 and 90 days were 0.9333, 0.95, 0.903 and 0.94, respectively. The correlation coefficients for the predicted flexural strength was measured for 3, 7 and 28 days were 0.86, 0.87, and 0.87, respectively.

For Geopolymer concrete durability permeability at (90 curing days) has been collected to predict correlation coefficients, which equal to 0.97.

Furthermore, despite differences in findings, the presented models showed to be a helpful tool in forecasting compressive strength of various geopolymer concretes. Those based on artificial neural networks outperformed models based on linear regression model. The use of an artificially neural networks to forecast compressive strengths in additives concrete at different curing durations has a great deal of potential in aspects of linear equations, and it's especially good at determining non - linear trends and relationships that are difficult to calculate with traditional techniques.

# Contents

Abstract.....	I
Contents.....	III
List of Figures .....	VI
Chapter One .....	1
Introduction.....	1
1.1. Background .....	1
1.1. Mineral Admixtures.....	3
1.2. Benefits and Drawbacks of Geopolymer Concrete .....	5
1.2.1. Geopolymer Concrete’s Benefits .....	6
1.2.3. Geopolymer Concrete’s Drawbacks .....	7
1.3. Study Objectives.....	8
1.4. Study Outlines .....	9
Chapter Two .....	10
Literature Review .....	10
2.1 Chemical Reaction of Mineral Admixtures with OPC .....	10
2.2 Environmental issues of Cement Production .....	10
2.3 Fresh Properties of Geopolymer Concretes .....	12
2.4 Mechanical Properties of Geopolymer Concretes .....	14
2.4.1. Compressive Strength.....	17
2.4.2. Splitting Tensile Strength and Flexural Strength .....	20
2.4.3. Modulus of elasticity and Poisson’s Ratio .....	21
2.5. Shrinkage Properties for Geopolymer Concrete .....	22
Chapter Three.....	24
Methodology.....	24

---

**Content**

---

.3.2	Statistical Analysis .....	25
3.2.1.	Non-Linear Regression modelling .....	25
3.2.2.	The Criteria of Efficiency .....	25
3.2.2.1.	Determination Coefficient (r).....	25
3.2.2.2.	Mean Absolute Error (MAE) .....	25
3.2.2.3.	Root Mean Square Error (RMSE).....	26
3.3.	Artificially Neural Networks Approaches (ANN) .....	26
3.3 Models	Structure of ANN .....	27
3.3.1.	Input layer .....	29
3.3.2.	Hidden layer .....	30
3.3.3.	Output layer.....	30
3.4.	Performance Criteria.....	31
3.4.1.	Root Mean Square Error (RMSE).....	32
3.4.2.	Mean Absolute Error (MAE) .....	32
4.1.	General.....	33
4.2.	Statistical Parameters.....	33
4.3.	Fresh Properties of Geopolymer Concrete (GPC).....	35
4.4.	Hardened Geopolymer Concrete's Mechanical Features .....	38
4.4.1.	Compressive Strength.....	38
4.4.2.	Splitting Tensile Strength .....	44
4.4.3.	Flexural Strength .....	49
4.4.4.	Dry Shrinkage Results .....	53
4.4.5.	Permeability Results .....	59
Chapter Five	.....	62
Conclusions and Recommendations	.....	62
5.1 General	.....	62
5.2 Conclusions	.....	62

---

**Content**

---

5.3 Recommendations For The Future Works ..... 63

Reference ..... 64

**List of Figures**

<b>Figure No.</b>	<b>Page No.</b>
Figure (2.1) Flowchart of pollutant and recycling of waste materials	12
Figure (3.1) Analyzing flowchart.	23
Figure (3.2) Section in neural network explains neural reading	28
Figure (3.3) Learning configurations settlements.	28
Figure (3.4) Sample of learning configurations bound values.	29
Figure (3.5) Flow chart of the study methodology for predicting geopolymer concrete properties	31
Figure (4.1) Slump results for Geopolymer concrete by SPSS.	36
Figure (4.2) ANN structure of Slump results prediction.	36
Figure (4.3) ANNs Weight Distribution of the succeeded model for Slump results.	37
Figure (4.4) Slump results for Geopolymer concrete by ANN.	37
Figure (4.5) Compressive Strength for Geopolymer concrete by SPSS at 3, 7, 28 and 90 curing days.	41
Figure (4.6) ANNs Weight Distribution of the succeeded model for Compressive Strength	41
Figure (4.7) ANN structure of Compressive Strength prediction	42
Figure (4.8) Compressive Strength for Geopolymer concrete by ANN at 3, 7, 28 and 90 curing days	43
Figure (4.9) Splitting Tensile Strength for Geopolymer concrete by SPSS at 3, 7, 28 and 90 curing days.	46
Figure (4.10) ANN structure of Splitting Tensile Strength prediction.	47
Figure (4.11) ANNs Weight Distribution of the succeeded model for Splitting Tensile Strength	47
Figure (4.12) Splitting Tensile Strength for Geopolymer concrete by ANN at 3, 7, 28 and 90 curing days.	49
Figure (4.13) Flexural Strength for Geopolymer concrete by SPSS at 3,	51

## List of Figure

---

7, and 28 curing days.	
Figure (4.14) ANN structure of Flexural Strength prediction.	51
Figure (4.15) ANNs Weight Distribution of the succeeded model for Flexural Strength.	52
Figure (4.16) Flexural Strength for Geopolymer concrete by ANN at 3, 7, and 28 curing days	53
Figure (4.17) Dry Shrinkage results for Geopolymer concrete by SPSS at 3, 7, 28 and 90 curing days	56
Figure (4.18) ANN structure of dry Shrinkage prediction	57
Figure (4.19) ANNs Weight Distribution of the succeeded model for Shrinkage results.	57
Figure (4.20) Dry Shrinkage results for Geopolymer concrete by ANN at 3, 7, 28 and 90 curing days.	59
Figure (4.21) Permeability results for Geopolymer concrete by SPSS at 90 curing days	60
Figure (4.22) Permeability results for Geopolymer concrete by ANN at 90 curing days	61

# Chapter One

## Introduction

### 1.1. Background

Joseph Davidovits and French scientists used the term "geopolymer" in the 1970s to describe a category of source materials created by reacting an alkaline solutions with an aluminosilicate powders (Davidovits, 1991). Because of diversity of formulations, geopolymer is known by many distinct names, including inorganic polymers and alkali-activated materials (AAM). Some believe that geopolymers should be called alkali-activated binders with low calcium precursors including calcined clays and low-calcium fly ash (LCFA) (Davidovits & Davidovics, 1991; PSWM Duxson et al., 2007).

Geopolymer concretes technology entails the creation of more ecologically friendly waste-based concretes that might be a viable alternative to traditional concretes. Nevertheless, in order to generate acceptable early strengths qualities, conventional fly ash-based geopolymer concretes needs a high temperature curing process, that is a significant constraint for cast-in-place concretes applications. The majority of prior research on geopolymer concretes has been on the qualities of concretes that have been pre-hardened by thermal curing and/or harsh chemical remediation (for example alkali activation with concentrated sodium hydroxides (NaOH)). Burning coal fly ash is gotten a lot of interest among the several aluminosilicates that have been researched for geopolymerization (Khale & Chaudhary, 2007).

The use of industrial solid waste materials has sparked the advancement of geopolymers, principally to meet the growing environmental and economic issues that industry has in dealing with these wastes. The two primary solid alumino - silicate sources that were extensively explored to generate geopolymers seem to be burning coal blast furnace slag and fly ash. Owing to ever-increasing global energy demand and industrial activity, these would be industrial effluents products generated in vast amounts all over the globe. They're frequently placed in landfills, not that this is a long-term solution, particularly as environmental rules get more rigorous. Landfilling is not only expensive because of legal and logistical challenges, however it also has long-term ecological impacts. Toxic metals are often found in these kind of industrial wastes, which might also leach and contaminate underground water. For certain applications, geopolymerisation allows discarded dangerous chemicals to be converted into commercially viable products with equal or even better qualities than cement-based products (Bondar et al., 2011; Djwantoro et al., 2004; Xu et al., 2006). Geopolymerisation seems to be another effective method for immobilizing toxic metals in waste materials. (Zhang et al., 2008).

It is widely known that the manufacture of Portland cement (PC) necessitates a significant amount of energy and contributes around 7% of total carbon dioxide emissions in the environment. Approximately 50% of CO<sub>2</sub> has been directly emitted into the air in cement manufacturing when the limestone has been heated in the calcination process. Just 40% has been emitted into the environment as a consequence of the burning fuels to raise the temperature the rotary furnace, and the remaining 10% has been evaluated for quarrying and transportation (Mahasenan, Smith and Humphreys, 2003; Yu, 2019). Furthermore, one ton of cement requires approximately 2.8 tons of raw materials; this is a resource-depleting process

---

that consumes a vast number of natural materials including limestone and shale for the manufacturing of cement clinkers (Guo et al., 2010). Moreover, the concrete industry requires around one trillion litres of adding water each year. In the same vein, behind the steel and aluminum industries, cement is among the most energy-intensive building materials, requiring roughly 110–120 kWh in a normal cement plant to manufacture one ton of cement (Mejeoumov, 2007).

Nonetheless, OPC cementing materials amount for the vast bulk of cementitious material used in concrete production. As a result, much research has been done to produce a new material that may be used as an alternative to OPC (Provis et al., 2015); geopolymer technology was developed initially by Davidovits in France in 1970. The high utilization of waste materials in the mixing ratio of geopolymer concretes (GPC) reduces greenhouse gas emissions by roughly 70% compared to PC concretes (Weil et al., 2009).

### **1.1. Mineral Admixtures**

To increase the quality of concrete, mineral admixtures are added. Rice husk ash (RHA), metakaolin (MK), ground granulated blasts furnaces slags (GGBS), silica fumes (SF), and Fly ashes (FA) are mineral additives that have varied qualities that impact the characteristics of concretes. Mineral additives' stated advantages are often linked to concrete's hardening qualities. Mineral additives, on the other hand, may change the characteristics of wet concretes in one or more of the following manner between blending and hardening: supply of water, hydration's heating setting time, bleed, and reactivity. There seems to be no literature that describes the influence of various mineral additives on the characteristics of new concretes, according to the researchers.

Furthermore, the impact of additives on the mechanical and durability characteristics qualities of concrete has remained an interesting topic. However, the impact of additives on the qualities of new concrete is critical, since these attributes might influence the concrete's mechanical and durability characteristics. The chemical product, mineral amount, shape, fineness, and glassy phase amount of these silica and alumina resources all influence their reactivity.

The raw materials must be extremely amorphous, have a suitable reactive glassy amount, have a low water requirement, and be able to release aluminum readily as the essential criteria for generating stable geopolymers. To activation alumino - silicate materials, alkali activators including potassium silicate ( $K_2SiO_3$ ), sodium silicate ( $Na_2SiO_3$ ), potassium hydroxide (KOH), and sodium hydroxide (NaOH) were utilized. When comparison to NaOH, KOH has a higher alkalinity level. However, it was shown that NaOH seems to have a larger capability for liberating silica and alumino monomers (Khale & Chaudhary, 2007). Geopolymer characteristics may be improved by selecting the right raw ingredients, mixing them correctly, and designing the processes to fit the purpose (Peter Duxson et al., 2007). Given the relevance of the topic, Italy, Spain, and France collaborated on the creation of a "Cost-effective geopolymeric cement for benign stabilization of hazardous components (GEOCISTEM)", which was funded by the European Commission. The goal of the experiment was to make geopolymeric cement by substituting potassium silicates with less expensive alkali volcanic tuffs (Davidovits et al., 1999). The solid alumino-silicate powders reactions with alkaline hydroxide/alkali silicate produces geopolymers.

A variety of variables impacted the mechanical properties of Geopolymer Concrete (GPC). The kind of an alkaline activators, its amount, and the curing temp all have a substantial impact on the development of mechanical strengths (Falah et al., 2020). The kind and amount of activator may affect workability and strength development. When comparison to OPC mortar (OPCM), geopolymer mortar (GPM)-based slag reacted by  $\text{Na}_2\text{CO}_3$  and NaOH produced excellent early strength, however the 28-day strength has been reduced. The GPC-based slag shrinkage triggered by such a high liquids sodium silicate amount was much greater than that of OPCC.

At room temp, water cured GPC-based slag had greater early strength than OPC (Collins & Sanjayan, 2002). The GPC-based fly ash shows low strength and the slow strength has been achieved once treated at the room temp. The geopolymerisation process and, as a result, the mechanical characteristics of GPC are improved by heat curing. The GPC-based fly ash strength may be increased by heat curing for a long time and at a high temperature. Although heat curing for GPC-based slag accelerates strength increase in the early stages, it results in lesser strengths at a later stage than samples treated at room temp. This is related to the rapid pace of reactivity that might have serious consequences including increased shrinkage and reduced strength.

## **1.2. Benefits and Drawbacks of Geopolymer Concrete**

Geopolymer concretes seems to be a cutting-edge material, which may be utilized in transportation infrastructures, specific projects, and offshore structures instead of typical Portland concrete or cement. It is extremely resistant to a number of the difficulties, which lead to create standard concretes to crumble and cracking. This is done by employing natural materials that have been little treated or industrial waste.

Portland concretes take longer to cure than geopolymer concretes. During 24 hours, they had gained the majority of their strength. This post will go over some of the primary advantages and disadvantages of geopolymer concretes.

The main benefits and drawbacks of Geopolymer concrete were presented (Neupane et al., 2018):

### **1.2.1. Geopolymer Concrete's Benefits**

It was a modern substance that makes typical concretes seem less impressive. Here are a few of the most significant benefits of geopolymer concretes.

- 1. High Strength:** It does have a good compressive strength, which is greater than conventional concrete. It also has a short strength development and cure time, making it a great choice for speedy builds. The tensile strength of geopolymer concrete is quite high. It is less brittle and therefore can sustain greater movement than Portland concrete. It isn't totally earthquake resistant, but it does hold up better than typical concretes in the event of an earthquake (Reddy et al., 2016).
- 2. Very Low Creep and Shrinkage:** The dry and heat of the concrete, as well as the water evaporates from the concrete, may generate serious and potentially deadly fissures in the concrete. Geopolymer concrete should not need hydration, is less porous, and shrinks less than ordinary concrete (Wallah, 2009). The creep rate of geopolymer concrete is exceedingly low. In layman's terms, creep refers to a concrete's propensity for being irreversibly warped as a consequence of continual stresses.

3. **Resistant to Heat and Cold:** It can resist temps of above 2200°F without losing its stability. Concrete may spall or have layers break apart due to excessive heating, lowering its stability. Spalling in geopolymer concrete does not happen until temps above 2200°F. It has developed a resistance to freezing in cold weather. Even though the pores are so small, water might still pass through hardened concrete. Water freezes and expands as temperatures dip below zero, causing cracks to develop. Geopolymer-based concrete would not freeze (Zhao & Sanjayan, 2011).
4. **Chemical Resistance:** It is chemically resistant to a high degree. Geopolymer concretes is unaffected by acids, hazardous waste, or salt water. Corrosion seems to be unlikely to develop with this concretes in the same way as it does with ordinary Portland concretes (Kurtoglu et al., 2018).

### 1.2.3. Geopolymer Concrete's Drawbacks

Despite the fact that geopolymer concretes seem to be the super concretes that will ultimately replace conventional Portland concrete, they do have some disadvantages:

1. **Difficult to Create:** Geopolymer concretes have unique handling requirements and is highly difficult to produce. It necessitates the use of potentially toxic chemicals, including sodium hydroxide (Masoule et al., 2022).
2. **Pre-Mix Only:** Owing to the hazards of making geopolymer concretes, it is only available as a pre-cast or pre-mixed product (Harrison & FCPA, n.d.).

3. **Geopolymerization Process is Sensitive:** This area of research has shown to be inconclusive and very turbulent. It seems to be a lack of consistency (Masoule et al., 2022).

Despite the fact that the notion of geopolymer concrete appeared to be fantastic and may be the finest thing to occur to concrete because Portland, there have been still too many unresolved issues that may cause major delays in the mixing and application process.

The importance of concretes properties may be an advanced method involving several external factors. Variety of improved prediction techniques are projected by together with empirical or process modeling, applied math techniques and computer science approaches. Several attempts are tested to mode this method throughout the employment of technique like finite part analyses. While, variety of analyses efforts focused on multivariable regression model to enhance the prediction accuracy. Applied math models can perform predictions faster than any other technique (Siddique et al., 2011). Hence, during last decades, many modeling depending upon Artificial Intelligence (AI) methods are presented, including fuzzy logic (FL), genetics algorithms (GA), and artificial neural networks ANN, which used in many engineering applications (Akkurt et al., 2004). Therefore, in this study new models for predicting the hardened and fresh properties of GC are presented.

### **1.3. Study Objectives**

This study is performed so as to present new predictive models to predict the engineering properties of the geopolymer concrete made with multi blended mineral admixtures. Also, in this study, an examination of the potential of statistical SPSS and ANN program in predicting of the

properties of the geopolymer concrete and mortar mixtures mineral admixtures is presented.

#### **1.4. Study Outlines**

This study consists of five chapters, these are:

**Chapter One:** includes general introduction, study objective and outlines.

**Chapter Two:** involves a review of relevant literature, material properties and effect of mineral admixtures.

**Chapter Three:** describes the methodology of the work. Such as, how the data is collected, establishment of the database, and data analysis using SPSS and ANN programs.

**Chapter Four:** demonstrates the results of the study and discussion.

**Chapter Five:** provides the conclusion of those study and recommendation are presented in chapter 5.

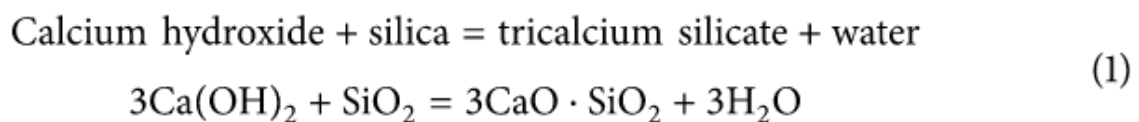
## Chapter Two

### Literature Review

#### 2.1 Chemical Reaction of Mineral Admixtures with OPC

The reaction of FA with ordinary Portland cement (OPC) takes place in two stages. The major reaction in the first step, throughout early curing, occurs with  $\text{Ca(OH)}_2$ ; nevertheless, the pace of reaction is dependent on the curing temp. The slower  $\text{Ca(OH)}_2$  activation at room temp slows down the response rate. The efficiency of using fly ashes in concrete is determined by a number of variables, involving the following: 1) the chemical and stage composition of OPC and FA; (2) the reaction system's  $\text{Ca(OH)}_2$  content; (3) the FA particle morphology; (4) the fineness of OPC and FA; (5) the formation of heating throughout the early hydrolysis reaction; and (6) the decrease in mixing water needs with FA.

Early stage characteristics and rheology of concretes are influenced by changes in FA chemical reactivity and composition (232, 2003). Durability, strength development, and With a constant supply of moisture, the lime interacts pozzolanically with the FA in the second step, producing additional hydration products with a fine pore structure. The pozzolanic response might well be described as follows:



#### 2.2 Environmental issues of Cement Production

The production of cement leads to the release of carbon dioxide into the atmosphere, resulting in contamination. Increasing demands on cement concrete's strength and longevity drive the use of admixtures, additives, or

both for particular applications. Geopolymer, an alternative binder made from highly concentrated aqueous alkali hydroxide or silicate solution and strong alumina silicate reactive elements, has the ability to reduce cement concrete's considerable carbon footprint (Assi et al., 2016; Mohammed & Fang, 2011; Vora & Dave, 2013).

The cement manufacture produces greenhouse gases both direct and indirect due to: limestone heating releases carbon dioxide, whilst fossil fuel combustion to heating the oven indirectly adds to Carbon dioxide and pollutant emissions.

- Calcination is a chemical process that results in direct cement emissions. Calcination occurs when calcium carbonate-based limestone is heated and decomposes into Carbon dioxide and calcium oxides. This process accounts for around half of all cement manufacture emissions.
- Indirect emissions are produced as a result of the burning of fossil fuels to heat the furnace. Furnaces were often powered by coal and natural gas, and the combustion of these fuels produces additional Carbon dioxide emission, just as it does in the creation of electricity. This accounts for around 40% of cement emissions. Finally, the energy used to power additional plant equipment and final cement transportation is an indirect emissions source that contributes for 5-10% of industry emissions.

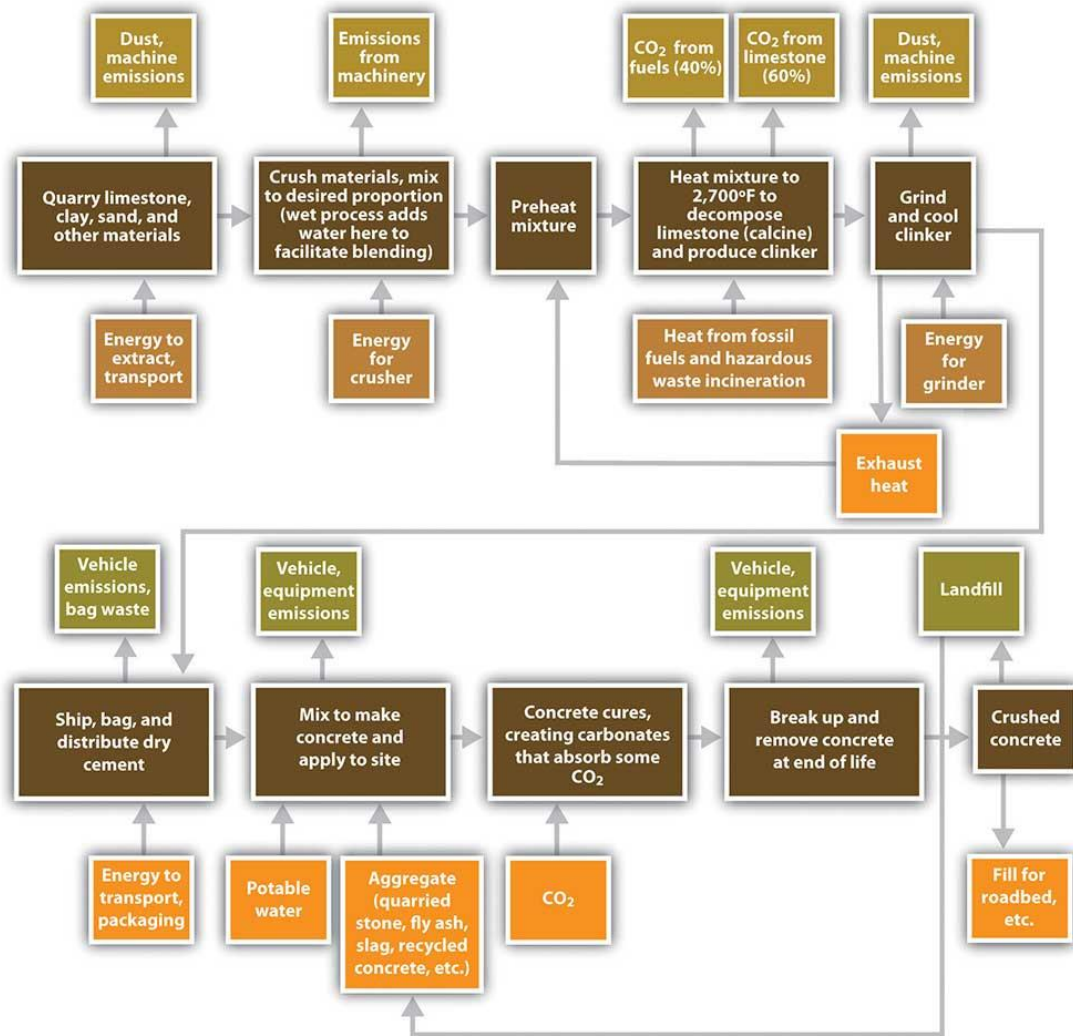


Figure (2.1) Flowchart of pollutant and recycling of waste materials (Shin et al., 2020)

### 2.3 Fresh Properties of Geopolymer Concretes

The viscosity and cohesiveness of fresh geopolymer concrete are very high, and it has a limited workability (Rangan et al., 2005). When water is added to fly ash-based concrete, it shows an extremely quick rate of chemical reaction, resulting in flash set in a matter of minutes, rendering it unusable (Cross et al., 2005).

Furthermore, increasing the quantity of rice husk ashes significantly enhanced the workability of new concretes, particularly in the coarser size

case. The results show that substituting rice husk ash for cement increases concrete's workability and compressive strengths while lowering its water permeability (Olivia, et al., 2008).

Chindaprasirt & Ridtirud, (2020) studied the usage of natural rubber latex as an ingredient in a high calcium fly ash geopolymer. The combinations included a great calcium fly ash geopolymer with natural rubber latex (medium ammonia concentration latex kind) contents of 0, 1, 2, 3, 5 and 10% by weight of fly ashes. Geopolymer mortars have been created for this project. For all mixes, the sand to fly ash proportion was 2.75, the liquid to fly ashes proportion was 0.6, and the  $\text{Na}_2\text{SiO}_3$  to NaOH proportion was 0.33. Surface abrasion resistant, flexural strengths, compressive strengths, apparent porosity, absorption, and Workability have all been evaluated. The test revealed that the optimal natural rubber latex concentration in geopolymer mortar had been 1.0 % by weight of fly ashes, resulting in enhanced mechanical qualities, a minor loss in workability, and a longer setting time. Increases in rubber particles, interface, and spacing between rubber particles and paste began to lower compressive strengths when more than 1% by weight of fly ashes latex was added.

Zhang et al., (2018) examined the properties of geopolymer mortars, including fresh performance (workability, setting time, and temp of fresh mortar), physical characteristics, mechanical characteristics (fracture behavior, bonding behavior, flexural performance, elastic characteristics, tensile strengths, and compressive strengths), durability characteristics (shrinkage characteristics, water absorption, frost resistant, resistant to high temperatures, and acid resistant), and migratability characteristics (acid resistant, resistant to high temperatures). The features of numerous kinds of geopolymer mortars made with diverse source materials as base materials are also discussed in this research. According to the present study's

---

findings, geopolymer mortar has shown substantial practicality and application potential as an environmentally friendly construction material that might eventually replace standard cement mortar.

Umniati et al., (2017) used retarder additive to improve the geopolymer concretes workability (Plastocrete RT6 Plus). The amount of retarder utilized ranges between 0.2 %, 0.4 %, and 0.6 % of the mass of fly ashes. Geopolymer concrete with no retarder (0 %) was also created as a control. The activator utilized in this study was  $\text{Na}_2\text{SiO}_3$  in a 1:5 proportion with NaOH 10 M solution. The findings revealed that a geopolymer concrete with 0.6 % retarder had the best composition, with an initial setting time of 6.75 hours and a final setting time of 9.5 hours. Furthermore, the droop of the geopolymer concretes has been 8.8 cm, with a 240 mm slump flow. The geopolymer concrete has a compressive strength of 47.21 MPa after 28 days. The experiment revealed that the more retarder applied to the geopolymer concretes, the longer it takes to set, enhancing its workability.

## **2.4 Mechanical Properties of Geopolymer Concretes**

Jindal, (2019) constantly studied to enhance the mechanical characteristics of geopolymer concretes and mortars while curing at room temp, in order to expand their use in building construction. The influence of different mineral additions on the microstructure, durability, and mechanical features of geopolymer concretes and mortars is summarized in this review study. Under normal temp settings, geopolymer products combined with these components exhibited a considerable increase in durability and mechanical characteristics. The findings suggest that geopolymer combinations with specified qualities might well be created for ambient temp curing using mineral additions, potentially promoting them as an ecologically friendly building material.

(Parveen and colleagues, 2019) The mechanical and microstructural features of the geopolymer paste created from industrial waste rice husk ashes (RHA) and ultra-fine slag are presented in this research. Slag particles that are ultra-fine, having an average particle size of 4 to 5 microns. RHA is partly replaced with ultra-fine slag at various amounts ranging from 0% to 50 Statistical Package for the Social Sciences. The proportion of sodium silicates to sodium hydroxide is 1.0, while the alkaline liquid to binder (AL/B) proportion is 0.60. With varied amounts of NaOH, the setting time, compressive, and flexural strengths have been examined up to the age of 90 days. SEM, EDS, and XRD on fractured specimens were used to investigate the microstructure of the composite geopolymer paste. High compressive and flexural strengths, as well as improved setting times, were achieved using a RHA-based geopolymer paste combined with ultrafine slag. At all ages, strength rose as the concentration of NaOH increased. The slag's ultra-small particles worked as a micro-filler in the paste, enhancing the characteristics by increasing CASH, NASH, and CSH. With 30 % slag concentration and 16M NaOH, the max compressive strengths of 70 MPa has been attained. The microstructure of the paste was densified by 30% substitution of RHA with ultra-fine slag, according to XRD, SEM, and EDS data.

He et al., (2013) Mechanical compression testing, X-ray diffraction, and scan electrons microscopy were used to evaluate the mechanical characteristics, microstructure, and geopolymerization responses of a different type of geopolymer composite made from two industrial wastes, red mud (RM) and rice husk ash (RHA), and the resulting samples were characterized by mechanical compression testing, X-ray diffractions, and scan electrons microscopy. Curing for a long time enhances compressive strength and Young's modulus while reducing ductility. Higher RHA/RM

---

proportions are associated with increased ductility, stiffness, and strength, but too much RHA might just have the reverse effect. The compressive strengths of the produced geopolymers with nominal Si/Al proportions of 1.68–3.35 varies from 3.2 to 20.5 MPa. The final products were often made up of an amorphous geopolymer binders with both inherited and neoformed crystalline forms as fillers, resulting in a composite with a complex composition and highly variable mechanical characteristics. Uncertainties in composition, microstructure, the amount of RHA dissolution, and reactions might be possible roadblocks to using RM–RHA based geopolymers as a building material.

Olivia et al., (2017) To get an excellent high strength, microstructure, and long-lasting product, geopolymer materials must be cured at a high temperature. In the case of cast in situ geopolymer, nevertheless, ambient temperature curing is preferred and practicable. The geopolymer is blended with calcium-rich mineral additives including slag, Ordinary Portland Cement (OPC), and high calcium fly ash to enable curing at room temp. Ordinary Portland Cement (OPC) was used in this work to induce setting and hardening of the Palm Oil Fuel Ash (POFA) geopolymer mortar at room temp. The POFA geopolymer mortar's setting time, compressive strength, and porosity have all been evaluated. 0 %, 20 %, 25 %, 30 %, 35 %, and 40 % OPC were added to the geopolymer. The alkaline activator employed was a mix of NaOH (16M) and Na<sub>2</sub>SiO<sub>3</sub> in a 2.5 mass proportion. At room temp, the POFA geopolymers mortar was cast and cured. At 28 days, adding 35 % OPC to mortar enhanced the setting time by 99.44 %, improved the compressive strength by 95.46 %, and lowered the porosity by 5.27 %. It may be inferred that adding OPC to the geopolymer material might increase its setting and ultimate strength.

### 2.4.1. Compressive Strength

This feature has been thoroughly researched in the lab, and the bulk of geopolymer concrete research papers included information on it. The parameters that control GPC's compressive strengths have been briefly addressed below. (Shehab et al., 2016) found that replacing 50% of ordinary Portland cement (OPC) with fly ash increased flexural strengths, splitting tensile strengths, bond strengths, and compressive strengths, whereas (Vijai et al., 2011) discovered that replacing 10% of fly ashes with OPC in GPC mixture risen flexural strengths, split tensile strengths, and compressive strengths. The addition of a 24-hour time before curing enhanced the GPC compressive strengths, according to (Lloyd & Rangan, 2009). When concretes is cured at room temp, it has a low early strength, however when it has been cured at high temp, it has a large strength increase. It must be mentioned that a longer curing time improves the geopolymerization process and, as a consequence, the concrete's strength; nevertheless, a longer curing time at a higher temp causes the concrete to fail. Compressive strength was often greater when the initial curing temp and time were higher.

The temp and time of initial heat curing have a crucial impact in the strength development geopolymer mortar-based fly ash, according to (Adam & Horianto, 2014). The best heat curing temperature has been determined to be 120 degree centigrade for 20 hours. According to (Joseph & Mathew, 2012), the ideal temp is 100 degree centigrade, whereas (Chindaprasirt et al., 2007) found that the optimum duration for curing at 60 degree centigrade is 3 h. The ideal curing temp, according to these experts, is 75 degrees Celsius. e response took 7 days to reach its max strength, and no additional strength has been seen. The significance of first heat curing has also been noted (Abdullah et al., 2011; Almuhsin et al., 2018; Vijai et

---

al., 2011). The compressive strength of concrete treated to one hour of furnace curing at 90 degree centigrade increased by 56 %, according to the latter study. Compressive strength was improved by increasing the heat curing period to 90 and 110 hours. (Görhan & Kürklü, 2014) looked at the time of heat curing and discovered that when heat curing (65 and 85 degree centigrade) has been extended from 5 to 24 h, compressive strength increased. Curing for more than 24 hours had no discernible influence on the strength.

Moreover, a range of ( $\text{Na}_2\text{SiO}_3/\text{NaOH}$ ) ratios have been utilized to make geopolymer concrete. For example, (Topark-Ngarm et al., 2015) employed a various proportion of  $\text{Na}_2\text{SiO}_3/\text{NaOH}$  and observed that compressive strength rose as the ratio of  $\text{Na}_2\text{SiO}_3/\text{NaOH}$  grew. According to Joseph and Mathew, the quantity of aggregate material in the geopolymer mixing ratios has an impact on the compressive strengths of the FA-GPC (Joseph & Mathew, 2012). They conducted an experimental lab study using various aggregate volumes ranging from 60% to 75% , and found that the FA-GPC with a total aggregates amount of 70 ercent, a sand-to-total aggregates proportion of 0.35, a molarity of 10, a l/b of 0.55, and a  $\text{Na}_2\text{SiO}_3/\text{NaOH}$  proportion of 2.5, once cured for 1 day at 100 , provided compressive strengths of 52 MPa.

According to tests conducted by (Kumar et al., 2017), the proportion of 7 days to 28 days compressive strengths of ternary mix GPC is between 88 and 90 %. Other experiments (Nguyen et al., 2020) found that 7 days could reach more than 93 % of the 28- day compressive strength, independent of fly ash kind, heating curing technique, or GGBS substitution. In contrast, measurements by (Chi, 2017) found that the proportion for mortar cure at 65 degree centigrade is 88 %, that is higher than the 66 % for regularly cured mortar. The compressive strength proportion of 7 to 28 days has been

---

determined to be 73 % and 88 % for the GPC-based metakaolin mixture exposed to typical air curing. Experiments on self-compacting GPC made of fly ashes and metakaolin reveal that the 7-day compressive strengths was comparable to the 28-day strength.

Depending on (Nguyen et al., 2020), increasing the water/solid proportion from 0.2 to 0.3 reduces the compressive strengths of FA-based GPC for alkali-to-binder proportions of 0.3 and 0.4, whereas tests by (Junaid et al., 2020) for GPC subjected to initial curing at 70 degree centigrade (Furnace) for 24 h revealed that the optimal water/binder proportion is 0.25 to reach optimal compress. When the alkali/fly ash proportions was increased to 0.45, which was less than 0.5, the strength increased (Abdullah et al., 2011; Mustafa Al Bakri et al., 2012). The optimal liquid alkali/fly ash proportions has found to be 0.4, whereas experiments by (Phoo-Ngernkham et al., 2018) show that raising the alkaline activators solution/fly ashes proportion from 0.4 to 0.9 reduces compressive strengths for both M10 and M15 NaOH solution. For GPC-based GGBS, optimum compositions of solid/liquid proportions has been indicated to be 3.0 specifying the proportion of 0.33 for the alkali/GGBS proportion.

The maximum compressive strength was observed in a NaOH solutions with a molarity of 12, whereas subsequent experiments revealed that the optimal molarity is 14. These findings contradict those of (Raijiwala & Patil, 2010), who found that a molarity of 16 yields the maximum compressive strengths. In comparison, (Samantasinghar & Singh, 2019) found that the maximal compressive strengths requires a molarity of 8.

(Jawahar & Mounika, 2016) discovered that the max compressive strength is connected to the use of GGBS, and that if this substance is partial replacement of natural with fly ashes, silica fumes, or metakaolin, there

---

seems to be a strength loss, or that if the basic Pozzolana is forced to replace with GGBS, there seems to be a strength enhancement. The later authors came to the conclusion that replacing fly ash with GGBS is a good alternative to oven curing. Almost identical results were achieved by (Saravanan & Elavenil, 2018). Slag's advantage over fly ash for GPC treated to various curing regimens had also been noted (Prakasam et al., 2020). In other studies, replacing up to 30% of the fly ash with GGBS resulted in a 30% improvement in compressive strength, independent of the curing temp. On the other hand, (Yunsheng et al., 2007) found that substituting 50% of metakaolin with GGBS resulted in the highest compressive strength. (Raut et al., 2019) obtained the same observation on geopolymer concrete with fly ash substituted by GGBS. Depending on (Okoye et al., 2016), substitute of fly ashes with silica fumes up to 40 % was found to be helpful to enhance compressive strength

It is indeed worth mentioning the impact of other variables on GPC strength. According to tests conducted by (Joseph & Mathew, 2012), the optimal overall aggregate is 70% and the fine/coarse aggregate ratio is 35% for a 0.55 alkali/fly ash mix. (Saini & Vattipalli, 2020) discovered that adding 2% nano silica to self-compacting GPC increased workability, mechanical performance, and durability. According to tests, replacing 5% of the GGBS with sugarcane bagasse ash (SCBA) results in the maximum modulus of elasticity, splitting tensile strength, and compressive strength. Compressive strengths of fly ashes GPC, on the other hand, enhanced as the calcium aluminate cement content increased.

### **2.4.2. Splitting Tensile Strength and Flexural Strength**

Indirect tensile strengths and flexural strengths were following the same pattern as GPC's compressive strengths, and generally, rising compressive

---

strength was associated with enhancing both flexural strengths ( $f_r$ ) and splitting tensile ( $f_{sp}$ ). The geopolymer concretes splitting tensile strengths has been just the compressive strength a fraction, according to (Rangan et al., 2005) test findings. There are, nevertheless, notable exceptions to the overall reaction indicated by certain researchers.

According to (Ryu et al., 2013), the tensile strengths rate growth slows as compressive strength increases. In contrast to compressive strength, substituting fly ashes with GGBS had a smaller influence on flexural and splitting tensile strengths. Experiments by (Oderji et al., 2019) revealed a decrease in flexural strength when the %age of fly ash replaced with slag went from 15 % to 20 %, despite the fact that this alteration improves compressive strength. In comparison to the modulus of elasticity of GPC, (Hassan et al., 2019) found that pre-heating concrete at 75 degree centigrade for 26 hours significantly improved compressive and flexural strengths. Other experiments (Saravanan & Elavenil, 2018) found that, in comparison to compressive strength, there might be a considerable increase in splitting tensile strength when 50% of fly ashes has been substituted with GGBS. The modulus of elasticity characteristic has been observed in the same way. When comparing the data provided by (Partha et al., 2013) to the data provided by others, it was discovered that utilizing a particular heat curing method increases the flexure/compression proportion while decreasing the tensile/compression proportion, as compared to ambient temperature curing.

### **2.4.3. Modulus of elasticity and Poisson's Ratio**

The modulus of elasticity ( $E_c$ ) of GPC follows the same trend as its compressive strengths, and depending on studies conducted by (Rangan et al., 2005), the modulus of elasticity of GPC increases as compressive strengths increases. The GPC modulus of elasticity is unaffected by the

---

curing process, according to (Nath & Sarker, 2017). In comparison to compressive strength, (Saravanan & Elavenil, 2018) found that when 50% of fly ash has been substituted with GGBS, the modulus of elasticity increases significantly.

In comparison to the other qualities, the Poisson's proportion has received less attention, and as a result, there is a scarcity of test data. Poisson's proportion magnitudes range from 0.23 to 0.26, which is somewhat higher than the magnitudes attributed to OPC-based concrete of normal strength. Other researchers discovered lower Poisson's proportion magnitudes for certain GPCs. Unlike the other qualities indicated, the GPC compressive strengths does not fluctuate on a regular basis. This feature decreases when compressive strength decreases, but (Sofi et al., 2007) observed that Poisson's proportion increases as compressive strength increases. Other studies reveal that, contrary to other GPC features, increasing the amount of fly ash replaced with GGBS reduces the Poisson's proportion. Overall, this tendency might make formulating formulas for forecasting Poisson's ration more difficult; nevertheless, this issue was resolved in the present study.

## **2.5. Shrinkage Properties for Geopolymer Concrete**

Concrete shrinkage occurs when the concrete's volume decreases over time. Shrinkage, unlike creep, is unaffected by the concrete's exterior activity. There are three forms of shrinkage, according to (Neville, 2000): drying shrinkage, carbonation shrinkage, and plastic shrinkage. Once concrete seems to be in a plastic condition as a result of evaporation or water suction by the underlying soil or concrete. Plastic shrinks with time. Carbonations happen once CO<sub>2</sub> from the atmosphere interacts with wet cement, causing shrinkage. Drying shrinkage is a reduction in volume resulted in water lossing from the gel pores throughout the drying process. Drying shrinkage

accounts for a large portion of overall long-term shrinkage. The volume and rate of drying shrinkage improvement are affected by the same parameters that impact concretes drying. The drying shrinkage is affected by the kind of cement, the amount of cement or binder, the amount of water, the water to binder proportion, the aggregates kind, and its size.

(Wallah, 2009) conducted research on Geopolymer concretes, using low-calcium fly ashes as raw materials, an alkaline solutions, and aggregates typically utilized in OPC concrete. Heatcured fly-ashes-based geopolymer concretes had a very low drying shrinking strain, researcher discovered. The drying shrinkage strains fluctuated somewhat over time, with a magnitude of roughly 100 micro strains after a year of testing. All test series of samples with varying compressive strengths that have been created from various blends and curing techniques, had no substantial differences after one year. The Gilbert Technique predicts magnitudes of drying shrinkage strain that are five to seven times greater than the actual drying shrinkage strain.

The shrinkage and microstructure properties of alkali-activation fly ashes/slag (AFS) mortars and pastes were studied by (Lee et al., 2014). Fly ashes, slag, and  $\text{Na}_2\text{SiO}_3$  have been mixed with distilled water to make the AFS mixes. Chemical shrinking of the alkali-activation fly ashes/slag paste was lower (0.06 0.10 mL/g) than that of the OPC paste, while autogenous shrink of the paste consists of AFS has been greater than those of the OPC paste. The overall porosity dropped as the slages or  $\text{Na}_2\text{SiO}_3$  concentration increased, and the mesopore volume fell at the same time, as the matrix got denser owing to the development of additional reaction products. The AFS mortar exhibited more drying shrink than the OPC sample, which might be due to the increased capillary stress induced by the AFS mortar's bigger mesopore comparison to the OPC mortar's.

---

## Chapter Three

### Methodology

In this chapter the following subjects will describe.

1. Flowchart
2. Collection of data
3. Analysis of data

The best way to understand the procedure used for designing the predictive model, is through the flowchart shown in Figure (3.1).

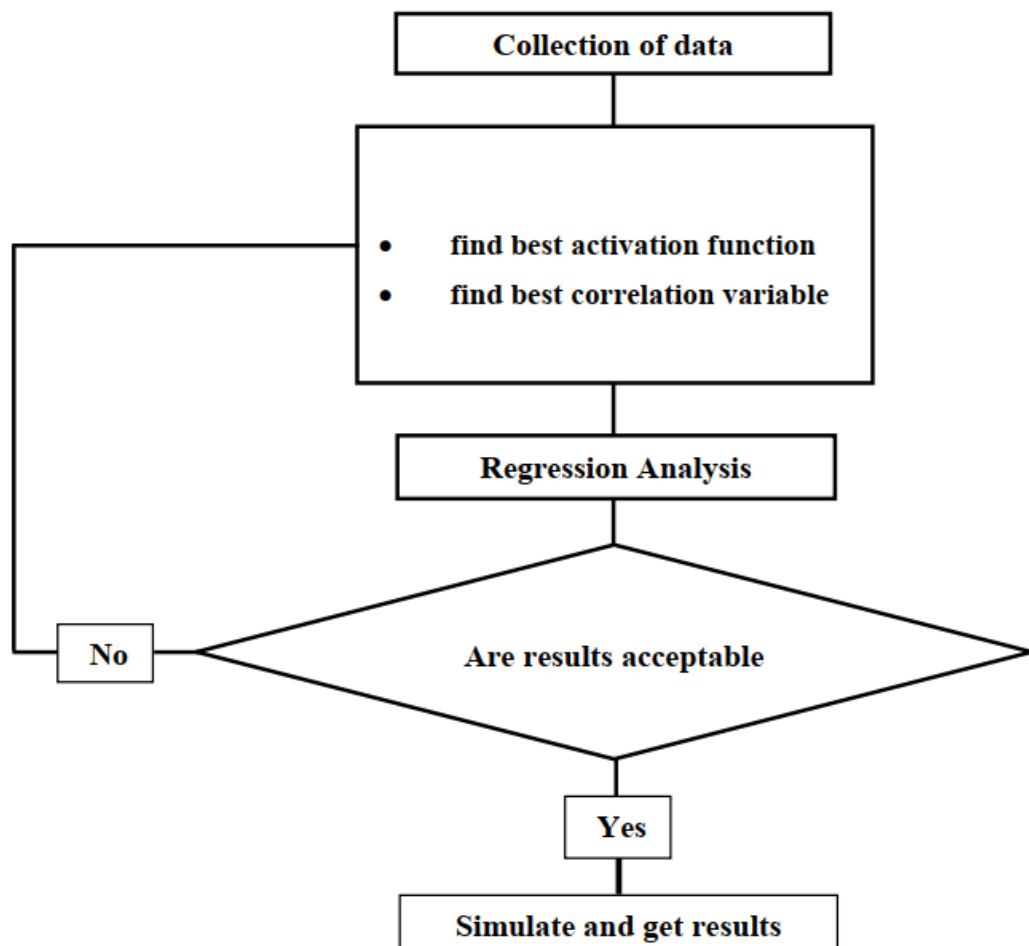


Figure (3.1) Analyzing flowchart

## 3.2. Statistical Analysis

### 3.2.1. Non-Linear Regression modelling

Statistical Package for the Social Sciences (SPSS) software is utilised for quantitative analysis and is utilised as a full statistical package depending on an interface point and click. From the data of creation in 1960 by Norman in cooperation with other programmers (Hadlai and Bent), this computer-programming has been commonly version 20 utilised by scientists to conduct quantitative analysis.

### 3.2.2. The Criteria of Efficiency

Presentation and evaluation of the effectiveness criteria utilised in this research. These are three criteria: determination's coefficient, Mean Absolute Error, and Root Mean Square Error to provide enough data on the errors of systematic in the simulation modelling as illustrated below.

#### 3.2.2.1. Determination Coefficient (r)

During this investigation, the determination coefficient,  $r$ , was written by:

$$r = 1 - \frac{\sum_{i=1}^n (y_b - y_p)^2}{\sum_{i=1}^n (y_b - \bar{y}_b)^2} \quad (3.1)$$

If  $r$  is 1.00, the model is treated as excellent (Erzin and Cetin, 2012).

#### 3.2.2.2. Mean Absolute Error (MAE)

The Mean Absolute Error MAE was represented by:

$$MAE = \frac{1}{n} \sum_{i=1}^n |y_b - y_p| \quad (3.2)$$

The above variables were utilised to evaluate the performance of the developed SPSS model. If MAE is equal to zero, the model is treated as excellent (Erzin and Cetin, 2012).

### 3.2.2.3. Root Mean Square Error (RMSE)

The mean root square error was written by eq. (3.3):

$$RMSE = \sqrt{\frac{\sum_{i=1}^n (y_b - y_p)^2}{n}} \quad (3.3)$$

Where RMSE is 0, the model is treated as excellent (Erzin and Cetin, 2014).

## 3.3. Artificially Neural Networks Approaches (ANN)

The artificially neural networks system (ANN) is amongst the most statistical procedures in the global, which can carry out the most complex problems with the goal that it would appear that the human brain and consist of various simple, profoundly interrelating preparing components, which procedure data by their dynamic condition response to exterior inputs. This system is based on a massive neural units that collection closely resembles how a real brain solves problems using a massive biological neurons collection linked by axons. ANN seems to be a mathematical model conducted by neurons; each node receiving input data, and that is the sum of the weights of previous neurons' outputs, and the neuron responds to this data input using a non-linear activation and biased magnitude. Artificial neural network system, generally, has 3 layers specifically, the input, hidden, and output layers. The input layer neurons receive input data from the exterior condition. Input layer does not play out any computations. Hidden layer neurons, which receive input data from the input layer performs calculation and gives the outputs to the output layer.

The output layer comprises of neurons that import the output of the network to the client or outside condition (Guo and Uhrig, 1992). In the ANN system, the number of hidden layers neurons decided from an experimentation procedure. If the neurons number in a hidden layer is excessively enormous, the approach will gain an overfit, i.e., the approach will have a problem in popularization. The datasets of training will be remembered and accordingly making the system useless on validation or testing stage. So as to developed (ANN) approach, many models of ANN were analyzed by alteration the number of hidden layers and the number of its neurons and the function of the training dataset (Beale and Jackson, 1990).

### 3.3 Models Structure of ANN

The structure of a neural number models may be stated as an ANN i-j-k, where I is the neural number of the input nodes, (j) is the neural numbers of the hidden layers, and (k) is the neural numbers of the output layers. The neural power program seems to be a neural artificially neural networks (ANN) that is used to calculate the bias and weights parameters that reduce mistakes in the output parameters. In order to obtain the input-output correlation, every procedure is provided a synaptic weight to indicate the proportional connecting strengths of 2 nodes at both sides. Figure (3.2) explains the neural network structure and shows the procedure of reading the neural and obtaining the corresponding neural number and its connections. The solution assumed to be reached the most suitable iteration. The learning and momentum rates are 0.8; learning configurations settlements and learning configurations bound values are shown in Figures (3.3) and (3.4).

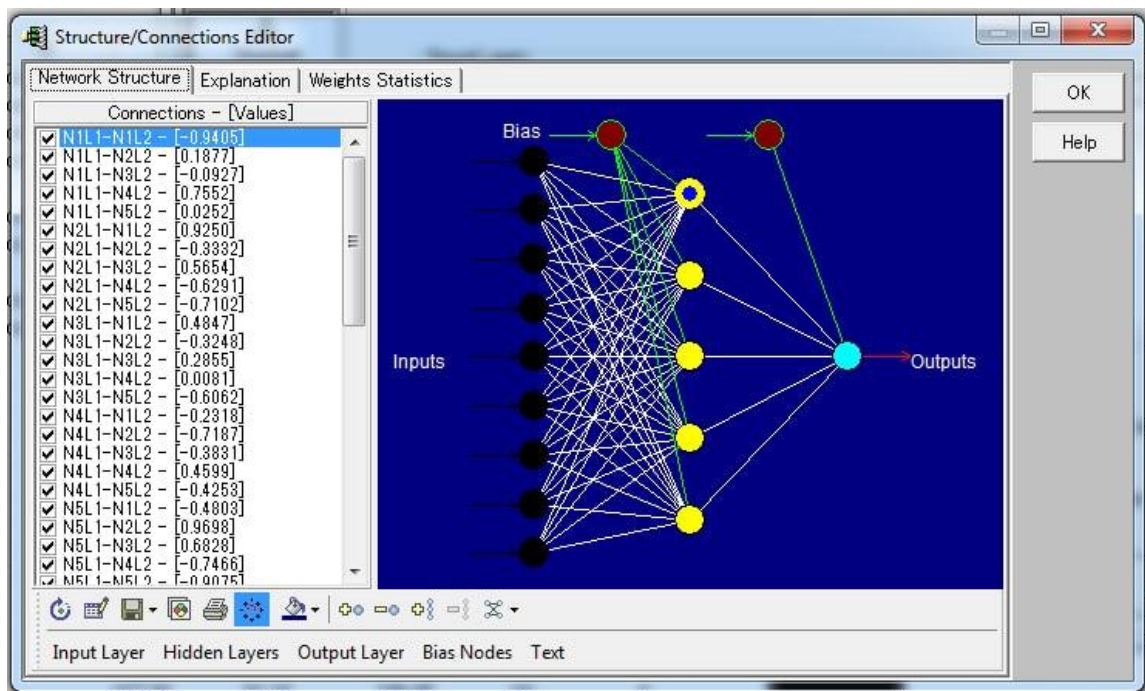


Figure (3.2) Section in neural network explains neural Reading.

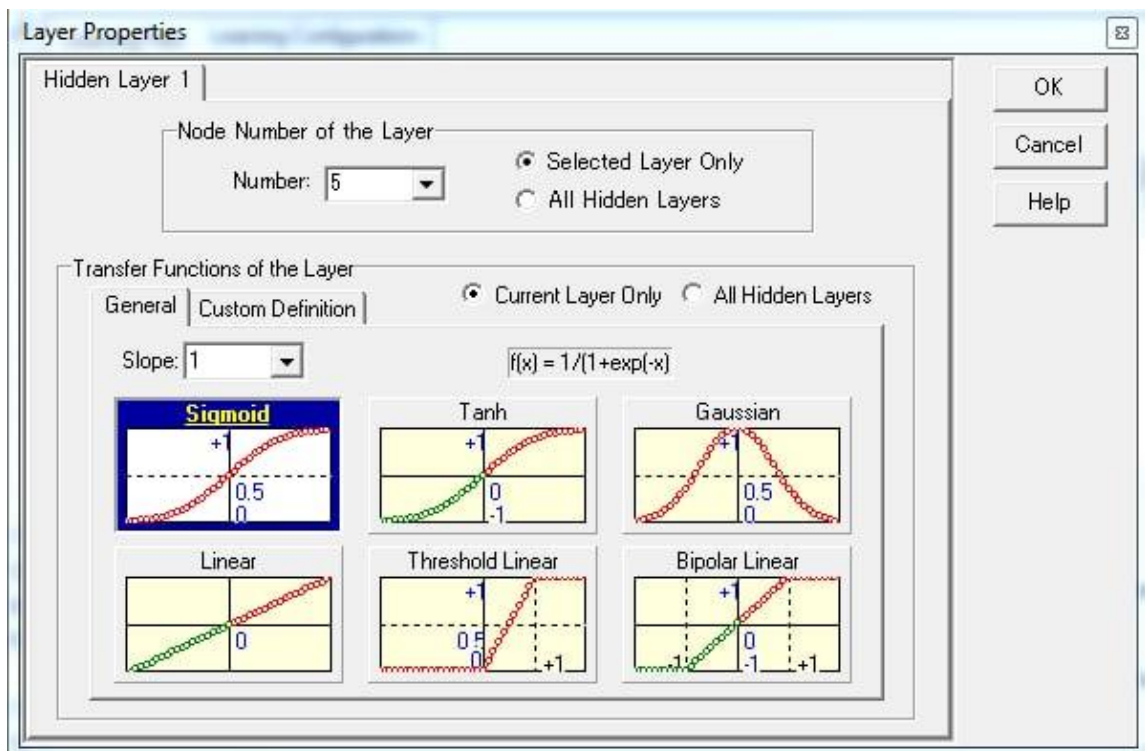


Figure (3.3) learning configurations settlements.

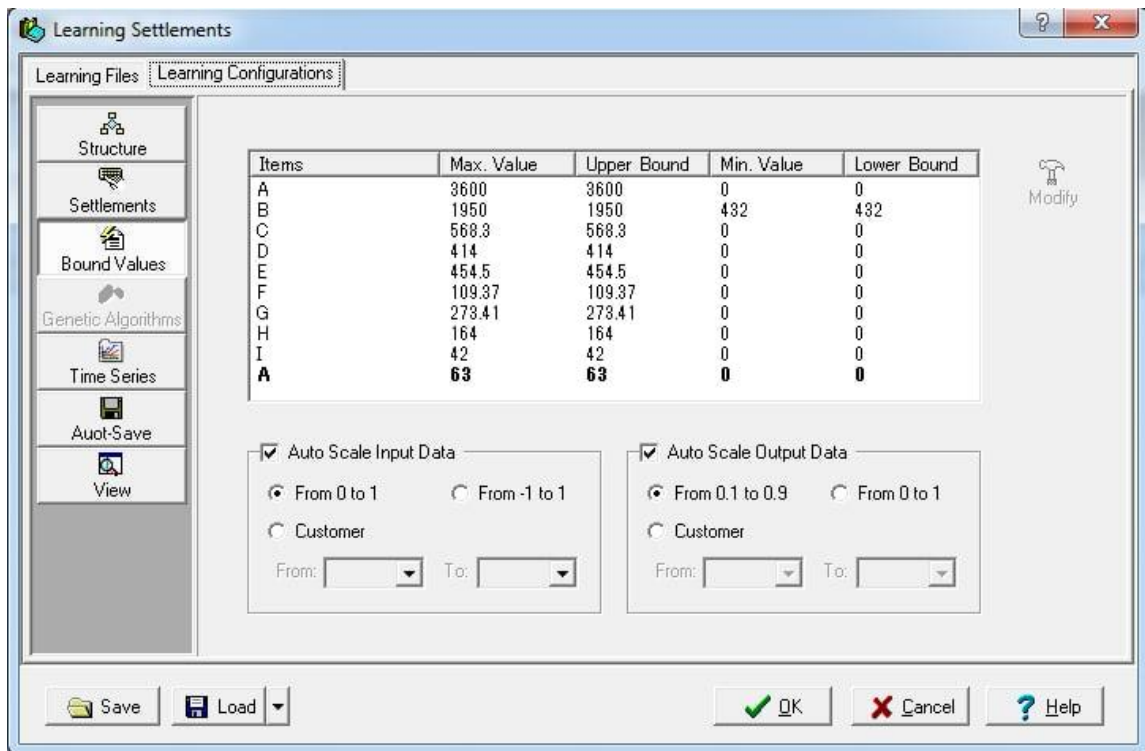


Figure (3.4) Sample of learning configurations bound values.

Because of the sigmoid function's behavior, the ANN output scale starts at zero and cannot exceed one; in these kind of instances, the data of the hidden layer and output layer must be scaled (CPC-X, 2003). Figure (3.5) shows a feasible strategy for developing neural predictions.

### 3.3.1. Input layer

The layer of input for all modelling based on the variables that are founded from data. The weight of input layer could be assumed up as follow:  $X_1$  is first variable's explanatory (H),  $X_2$  is ( $\alpha$ ),  $X_3$  is ( $\phi$ ),  $X_4$  is ( $X_c$ ),  $X_5$  is ( $Y_c$ ),  $X_6$  is the last variable's explanatory (R).

### 3.3.2. Hidden layer

The data relocation from the input layer to the hidden layer and process with functional activation and bias magnitude as displayed below:

$$Y_j = \beta_j + \sum W_{i,j} X_i \quad (3.4)$$

$$\sigma Y_j = \frac{1}{(1+e^{-Y_j})} \quad (3.5)$$

### 3.3.3. Output layer

This layer will receive and process then display the layer's hidden results as output neural system upshot as following:

$$Y_k = \beta_k + \sum W_{j,k} \sigma Y_j$$

$$\sigma Y_k = \frac{1}{(1+e^{-Y_k})} \quad (3.6)$$

Where:

$X_i$  = the variables of input,

$Y_k$  &  $Y_j$  = The magnitude of sigmoid function power output and input, respectively.

$\beta_k$  &  $\beta_j$  = layers' hidden and output bias magnitudes, respectively.

$W_{i,j}$  = the connection weights between input layer's neurons.

$W_{i,k}$  = the connection weights between layer's hidden neurons.

$\sigma Y_j$  &  $\sigma Y_k$  are upshot magnitudes of layers' output and hidden, respectively.

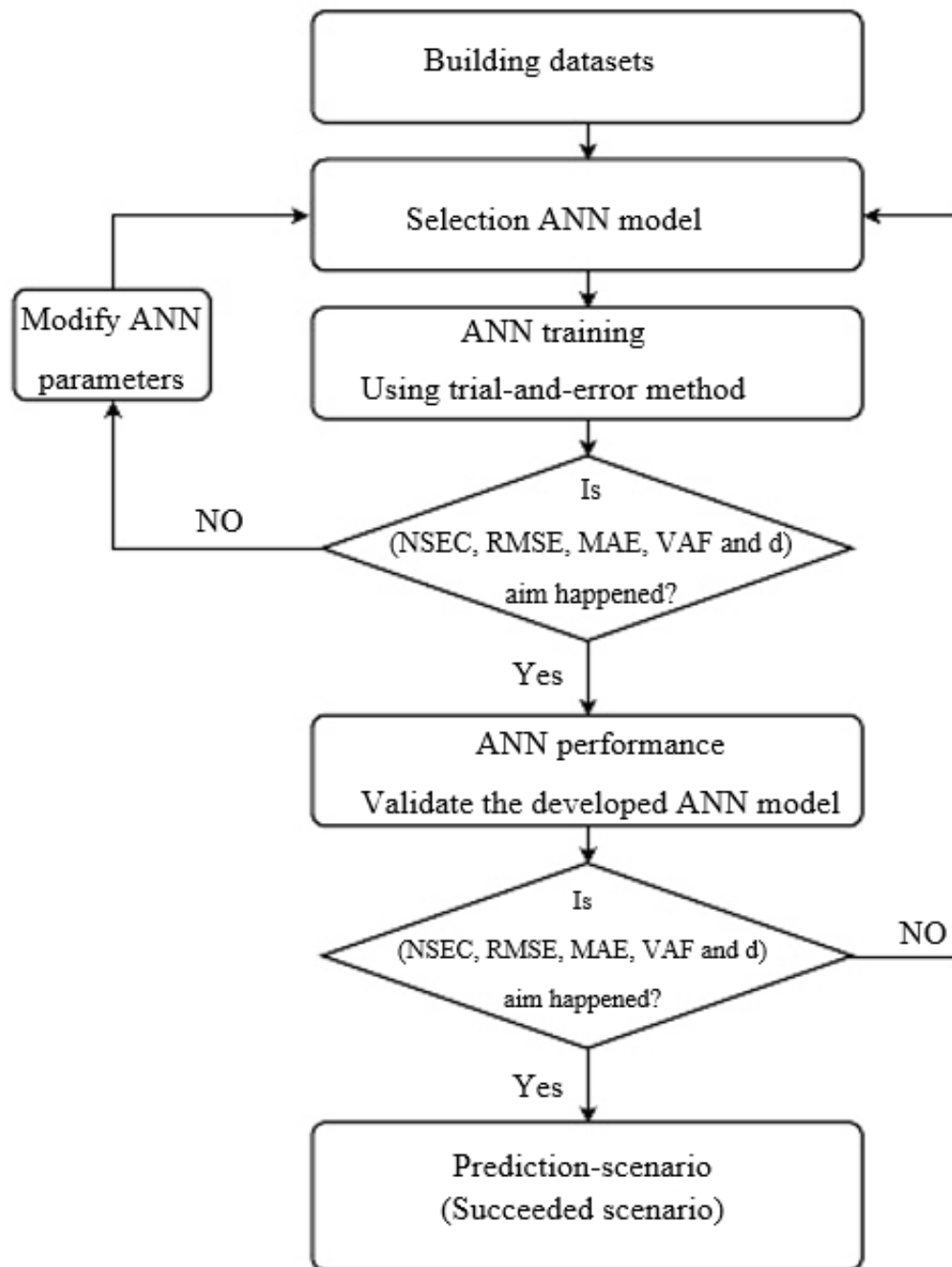


Figure (3.5) The methodology flow-chart for expecting geopolymers concrete properties

### 3.4. Performance Criteria

The procedure developed to evaluate the behavior of ANN design involves gaining the smallest statistics measuring of error between computed and

expected magnitudes. The coefficient of correlation (R2) between the computed and predicted magnitudes is a beneficial indicator to monitor the prediction performance of the model. In this study, to enumerate the agreement between computed and predicted magnitudes, we practiced 5 numerical events: Nash- Sutcliffe efficiency (NSEC); the absolute mean error (MAE); the error of root mean square (RMSE); Agreement Index (d); Variance (VAF).

The formulations for calculating the previous 5 statistical behavior criteria are stated as following:

### 3.4.1. Root Mean Square Error (RMSE)

The regularly utilized measure of the variances between magnitudes (sample magnitudes) expected by a modelling or an estimator and the observing magnitudes. It is calculated as:

$$RMSE = \sqrt{\frac{\sum_{i=1}^n (y_b - y_p)^2}{n}} \quad (3.7)$$

### 3.4.2. Mean Absolute Error (MAE)

Error of Mean Absolute is a metric evaluation modelling utilized with models of regression. The error of mean absolute of a model with respecting to a set of test is the mean's absolute magnitudes of the separate expectation errors over all examples in the group of test. Every expectation error is the difference between the true magnitude and the predicted magnitude for the example. It is calculated as:

$$MAE = \frac{1}{n} \sum_{i=1}^n |y_b - y_p| \quad (3.7)$$

## Chapter Four

### Results and Discussion

#### 4.1. General

As previously reported, study is performed so as to present new predictive models to predict the engineering properties of the geopolymer concrete, made with multi blended mineral admixtures. Also, in this study, an examination of the potential of statistical SPSS and ANN program in predicting of the properties of the geopolymer concrete and mortar mixtures multi blended mineral admixtures is presented. An analysis program has been undertaken to achieve this aim, as defined in chapter three. In this chapter, the test results are explored in terms of SPSS and ANN analysis to predict fresh and hard geopolymer concrete properties.

#### 4.2. Statistical Parameters

After supporting the SPSS program by all the variables needed in the multiple linear regression equation, the statistical parameters of the regression analysis ( $R$ ,  $R^2$ , adjusted  $R^2$ , standard errors) described in Table (4.1).

**Table 4.1 Statistical Parameters**

property	R	$R^2$	Adjusted $R^2$ the estimate	Standard error of the estimate
Slump flow (mm)	0.93690	0.8778	0.959	59.54859
Compressive strength (MPa) (3 days)	0.96953	0.94	0.938	70.543
Compressive strength (MPa) (7 days)	0.96436	0.93	0.927	5.48715
Compressive strength (MPa) (28 days)	0.9539	0.91	0.903	6.38385

Compressive strength (MPa) (90 days)	0.97979	0.96	0.96	4.50064
Splitting tensile (MPa) (3 days)	0.9660	0.9333	0.923	71.28
Splitting tensile (MPa) (7 days)	0.9746	0.95	0.943	0.48704
Splitting tensile (MPa) (28 days)	0.95026	0.903	0.932	9.54065
Splitting tensile (MPa) (90 days)	0.96953	0.94	0.995	0.17785
Flexural Strength (MPa) (3 days)	0.927362	0.86	0.427	6.132
Flexural Strength (MPa) (7 days)	0.932738	0.87	0.757	0.492
Flexural Strength (MPa) (28 days)	0.932738	0.87	0.729	2.529
Shrinkage (mm) (3 days)	0.942178	0.8877	0.809	0.418
Shrinkage (mm) (7 days)	0.942178	0.8877	1	0.001
Shrinkage (mm) (28 days)	0.943398	0.89	0.454	5.403
Shrinkage (mm) (90 days)	0.943398	0.89	0.969	0.00
Permeability (90 days)	0.984886	0.97	0.962	11.452

**1. Correlation Coefficient:** It measures the relations between variables. The value of correlation between negative and correct one

$$-1 \leq R \leq 1$$

When:

- |                     |                                    |
|---------------------|------------------------------------|
| a. $R = 0$          | No relation between variables      |
| b. $R =$ (positive) | strong relation between variables  |
| c. $R =$ (negative) | inverse relation between variables |

**2. Determination of Coefficient  $R^2$ :** This coefficient represent the %age of the independent variables contribution to explain the change in the dependent variables. Its normal value is (0 – 1).

**3. Adjusted Coefficient of determination (Adjusted  $R^2$ ):** It take into the number of independent variables.

**4. The standard error of regression, known also as (standard error of the estimation):** Represent the average distance that the actual value fall from the regression line.

### **4.3. Fresh Properties of Geopolymer Concrete (GPC)**

Workability of GPC mixes was studied using slump cone test. The fresh geopolymer concrete mixes were observed highly harsh and particularly in the case of GPC produced slump less concrete.

Figure (4.1) demonstrate the correlation between the slump from SPSS and slump from data for predicted slump, where the best model expression for the regression coefficient ( $R^2$ ) value was 0.8778. Figure (4.4) demonstrate the correlation between the slump from ANN and slump from data for predicted slump, where the best model expression for the regression coefficient ( $R^2$ ) value was 0.92. However, ANN present better regression coefficient comparison with SPSS results.

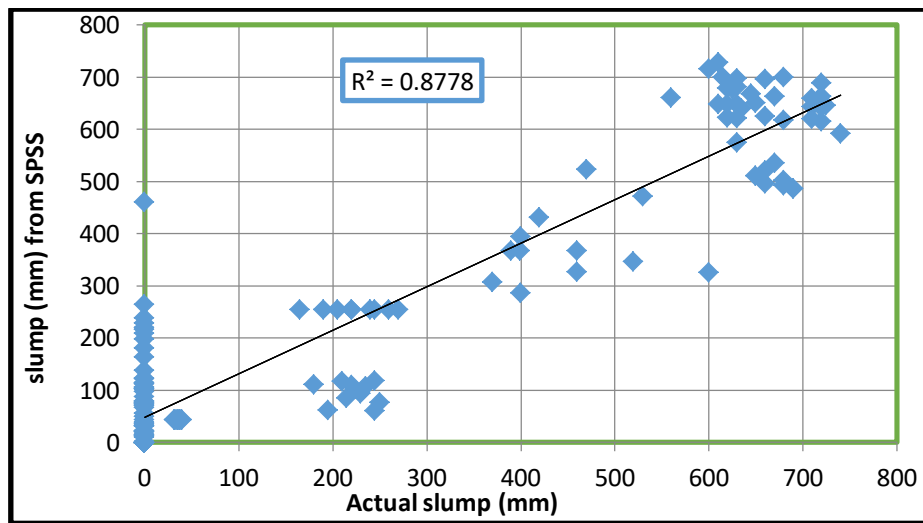


Figure (4.1) Slump results for Geopolymer concrete by SPSS.

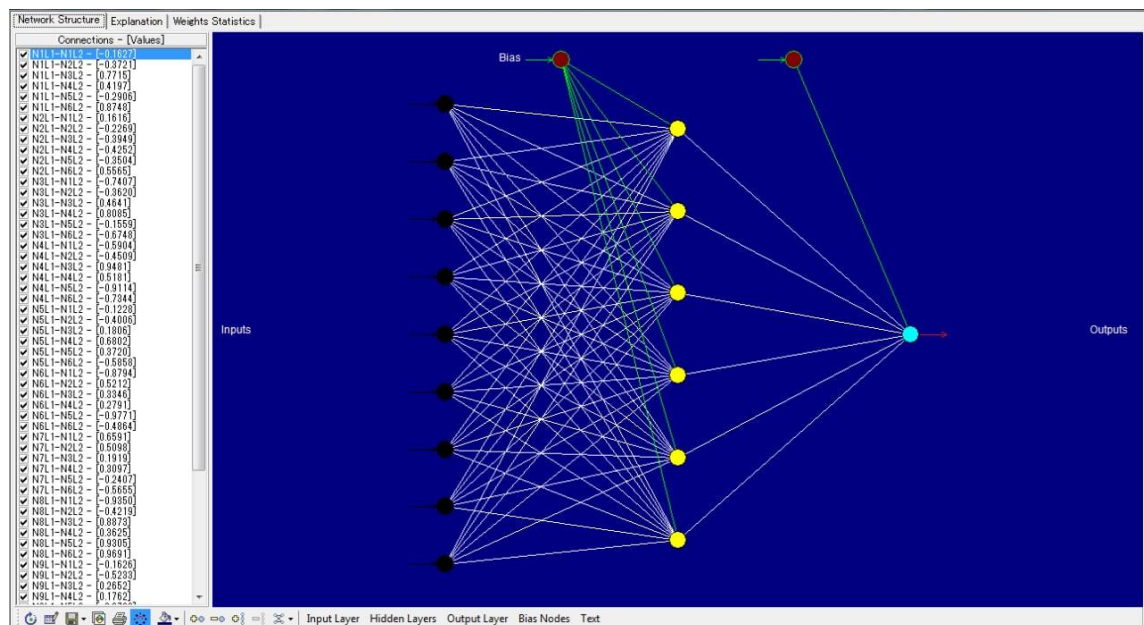


Figure (4.2) ANN structure of Slump results prediction.

The best ANN connections from the succeeded model are utilized to evolve the forecast models for Flexural strength as illustrated in Figure (4.24)

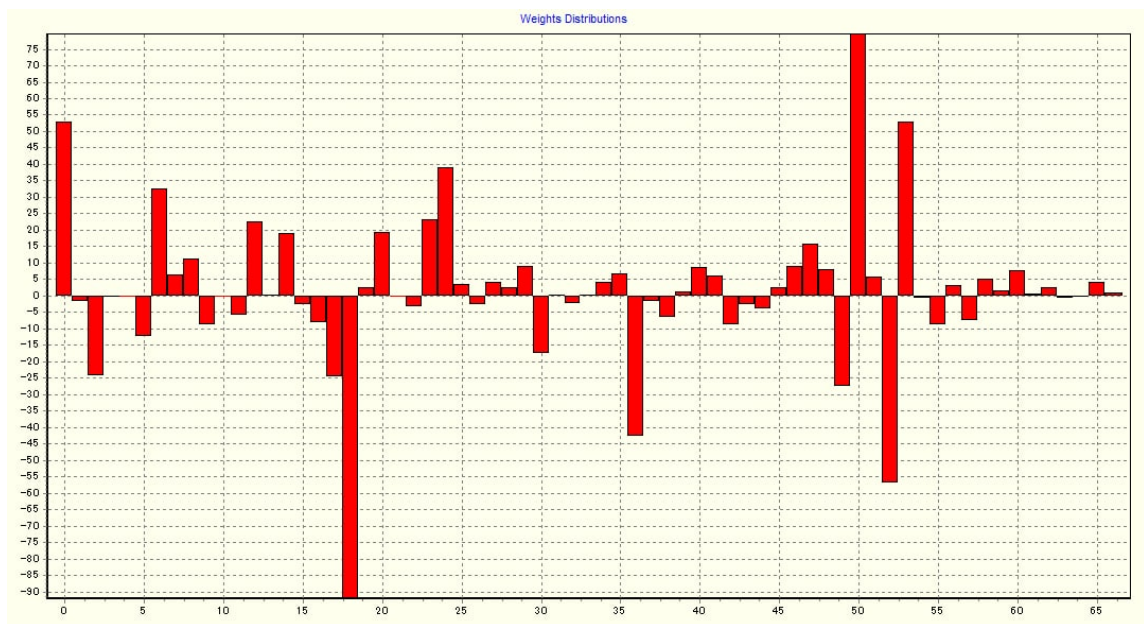


Figure (4.3) ANNs Weight Distribution of the succeeded model for Slump results.

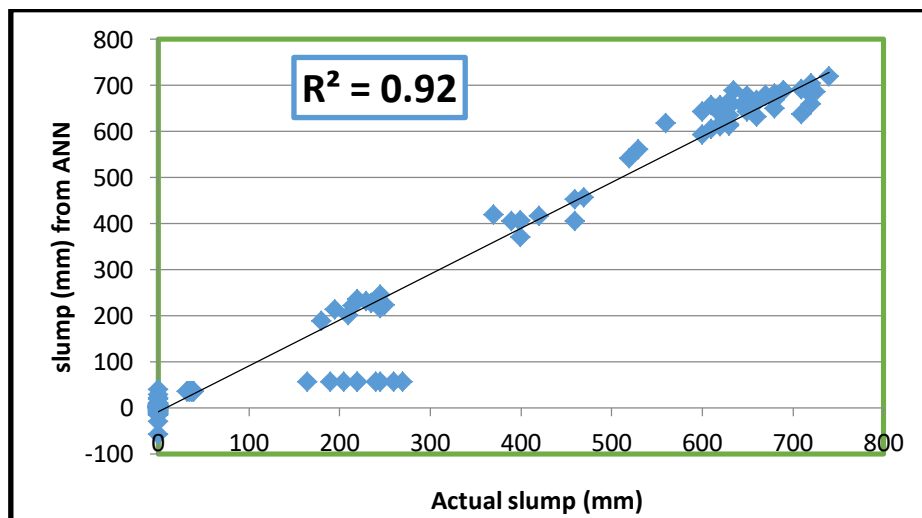


Figure (4.4) Slump results for Geopolymer concrete by ANN.

It can be noticed from Figure (4.3 and 4.4) that the correlation between the predicted and actual values obtained from the above equations for GPC slump flow property is always positive, where  $R$  is 0.933 ,  $R^2$  is 0.8715, and adjusted  $R^2$  is 0.83, which mean there is a strong relation between variables,

hence, the results obtained in this study agrees with results obtained by (Oyebisi et al., 2020).

#### **4.4. Hardened Geopolymer Concrete's Mechanical Features**

Understanding the behavior of geopolymer concrete with different minerals additives beam specimens requires a thorough understanding of its mechanical features. The strengths of compressive, splitting tensile, Flexural; and shrinkage are among the mechanical properties of hardened concrete predicted in this research.

##### **4.4.1. Compressive Strength**

The strengths of compressive for geopolymer concrete has been predicted by using statistical analysis (SPSS) and An artificial neural network (ANN). Figure (4.5) demonstrate the correlation between the compressive strength from SPSS and compressive strength from data for predicted compressive strength, where the best model expression for the regression coefficient ( $R_2$ ) value was 0.94. Figure (4.8) demonstrate the correlation between the compressive strength from ANN and compressive strength from data for predicted compressive strength, where the best model expression for the regression coefficient ( $R_2$ ) value was 0.9635. However, ANN present better regression coefficient comparison with SPSS results.

From (4.6) it can be seen clearly that the correlation between the predicted and actual values obtained compressive strength with age of 7 days are always positive, where  $R$  is 0.931 ,  $R^2$  is 0.867, and adjusted  $R^2$  is 0.8, which mean there is a strong relation between variables.

Finally, depending on mixture parameters, a multinomial model has been created to estimate the CS of additive concrete. Table 4.1 summarizes the

regression models by listing the statistical factors derived at the 95 % confidence level, which is a typically utilized level in statistical data analysis.

Predictive models of compressive strength(CS) , as derived by MRA, are as follows=

**For 3 curing days**

$$CS = -3.812CA - 0.242FA + 1.988FSH - 1.684GGB + 10.580SL - 0.164NH + 2.927NS + 2.682W + 2.371SP$$

- **For 7 curing days**

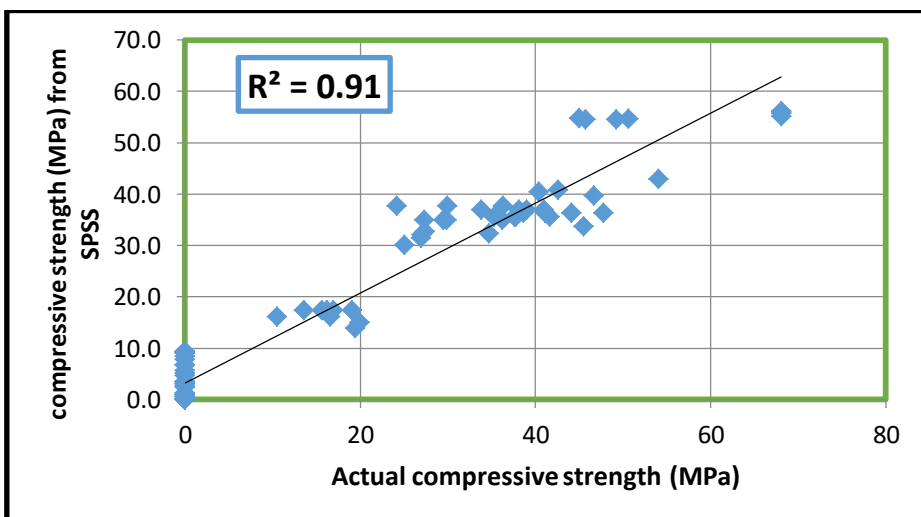
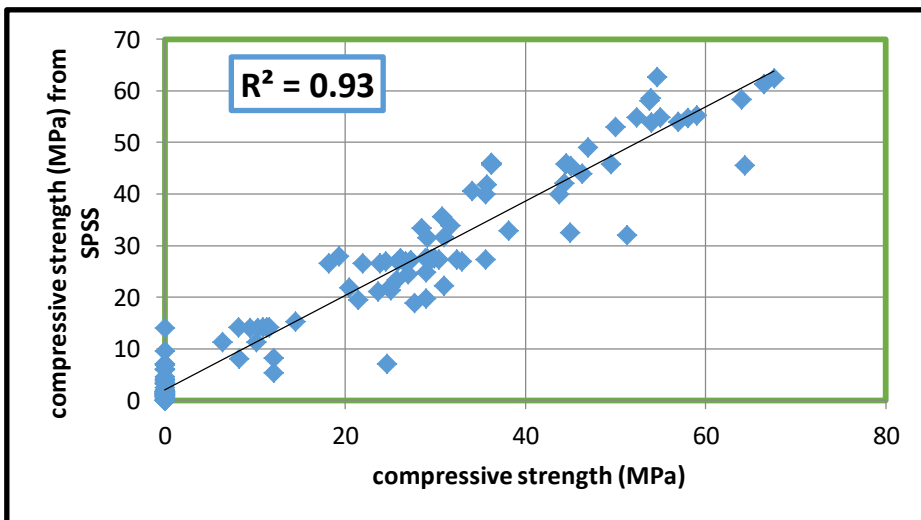
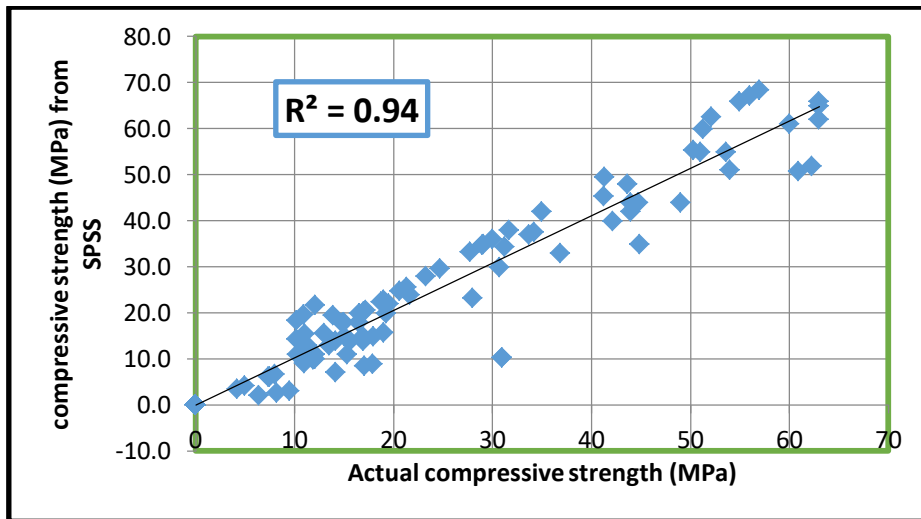
$$C.S = 0.939CA - 4.830FA + 7.877FSH - 1.217GGB + 4.574SL + 0.568NH + 6.948NS + 10.454W - 2.310SP$$

- **For 28 curing days**

$$CS = 8.365CA + 6.004FA + 0.774FSH + 0.536GGB - 0.191NH - 2.188NS + 1.028W - 1.903SP$$

- **For 90 curing days**

$$C.S = 2.302CA + 0.922FA + 1.1990FSH + 3.11GGB + 1.065NH + 0.862NS + 0.404W - 2.815SP$$



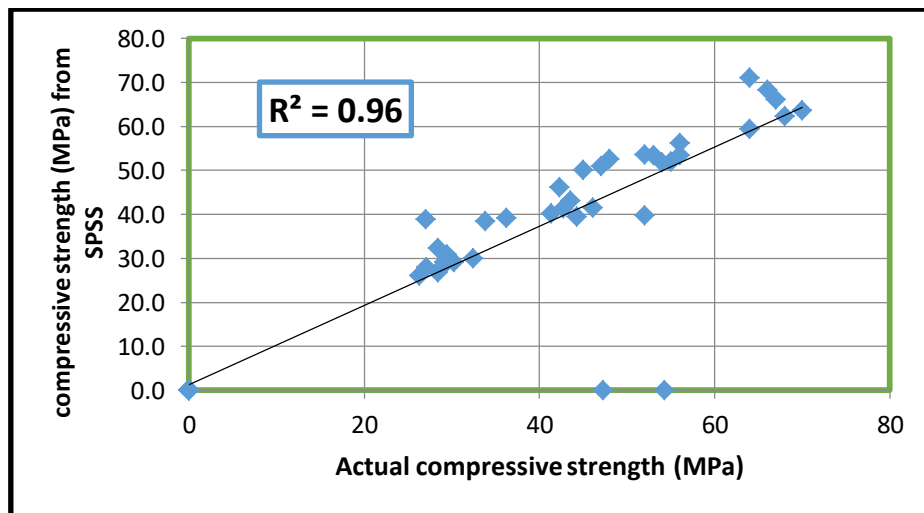


Figure (4.5) Compressive Strength for Geopolymer concrete by SPSS at 3, 7, 28 and 90 curing days.

The best ANN connections from the succeeded model are utilized to evolve the forecast models for Compressive Strength as illustrated in Figure (4.6)

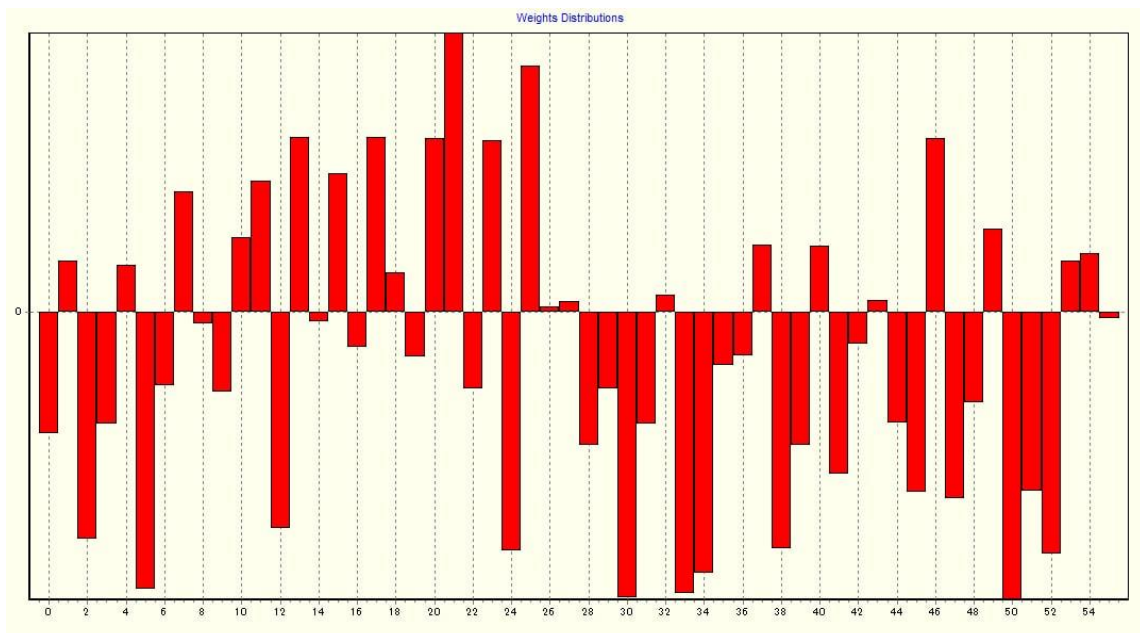


Figure (4.6) ANNs Weight Distribution of the succeeded model for Compressive Strength.

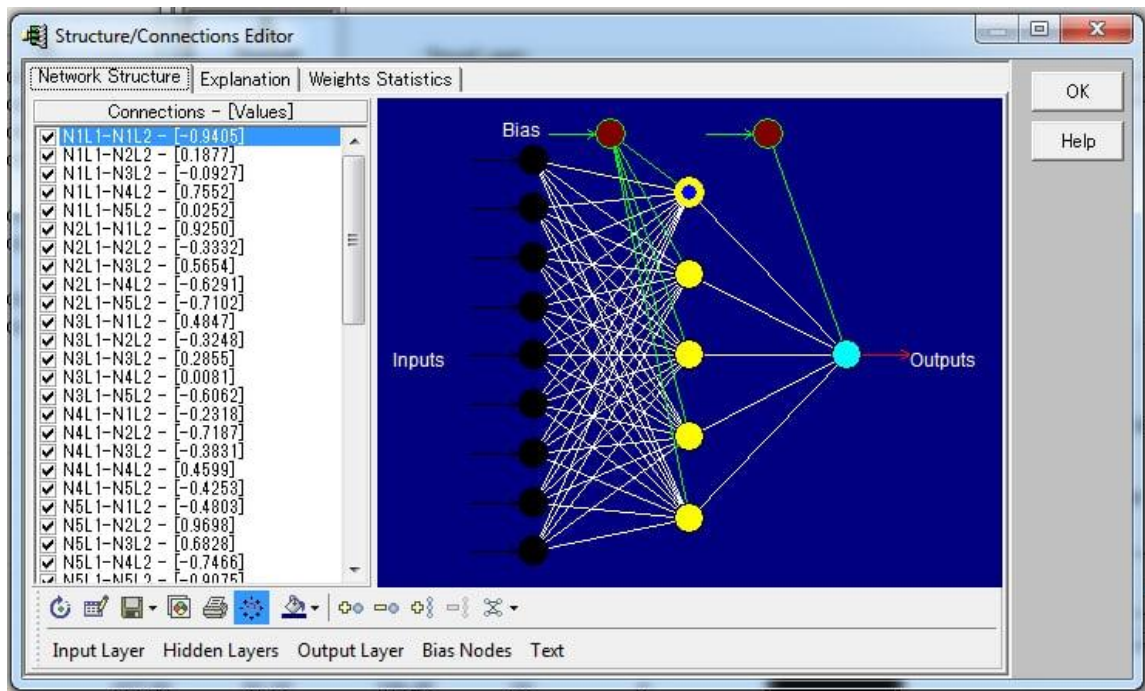
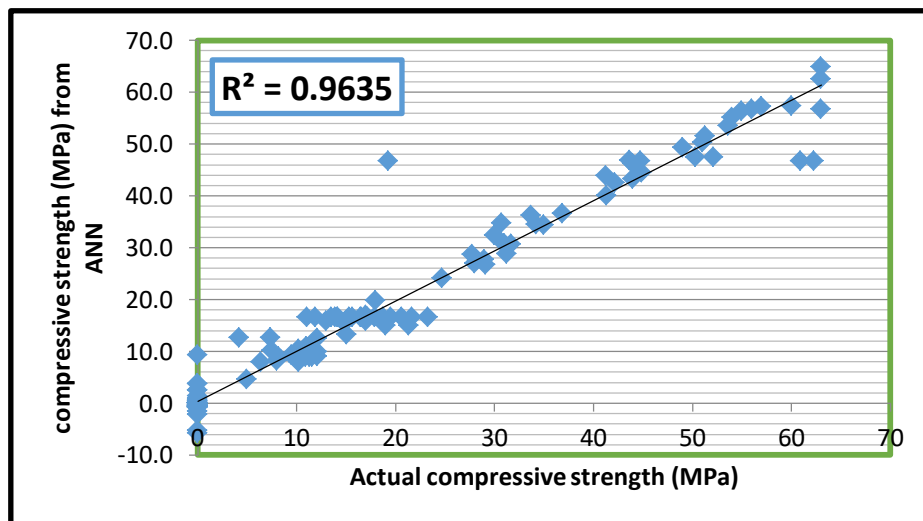


Figure (4.7) ANN structure of Compressive Strength prediction.



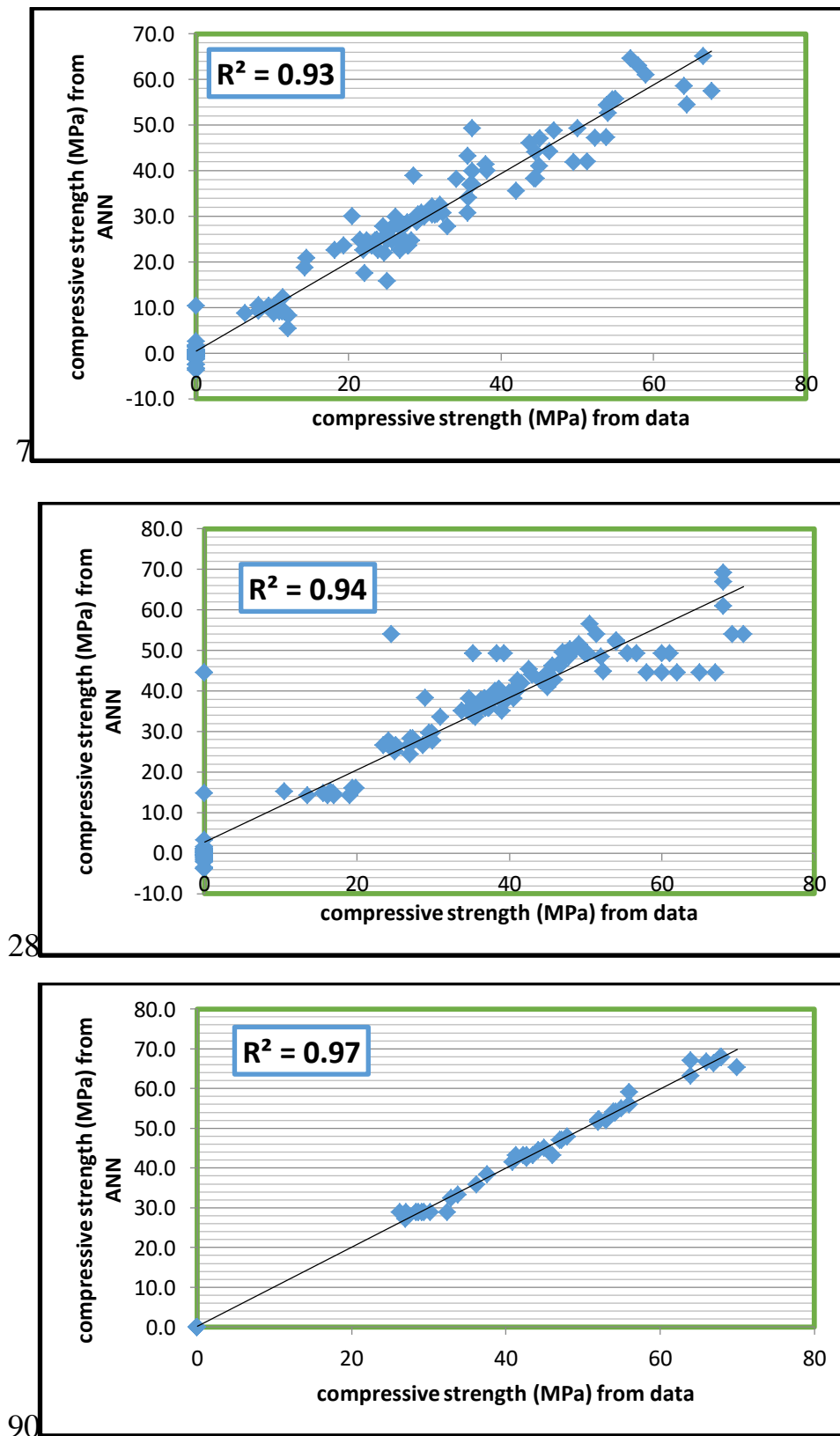


Figure (4.8) Compressive Strength for Geopolymer concrete by ANN at 3, 7, 28 and 90 curing days.

### 4.4.2. Splitting Tensile Strength

To be more explicit, data scattering of splitting tensile strengths for GPC exposed to initial heating curing or ambience curing must be shown, since the curing system has been discovered to have a significant impact on every mechanical characteristic, as several researchers have noticed. The strengths of Splitting Tensile for geopolymer concrete has been predicted by using SPSS and ANN statistical analysis. Figure (4.9) demonstrate the association between the Splitting Tensile Strengths from SPSS and Splitting Tensile Strength from data for predicted splitting tensile strengths, where the best model expression for the regression coefficient ( $R_2$ ) value was 0.95 for 7 curing days. Figure (4.12) demonstrate the association between the splitting tensile strengths from ANN and splitting tensile strength from data for predicted splitting tensile strengths, where the best model expression for the regression coefficient ( $R_2$ ) value was 0.9. However, SPSS present better regression coefficient comparison with ANN results.

Predictive models of Splitting, as derived by MRA, are as follows=

- **For 3 curing days**

$$\text{Splitting} = -0.449CA - 0.672FA - 6.020FSH + 2.372GGB - 6.504SL - 0.387NH - 2.575NS - 3.697W + 1.321SP$$

- **For 7 curing days**

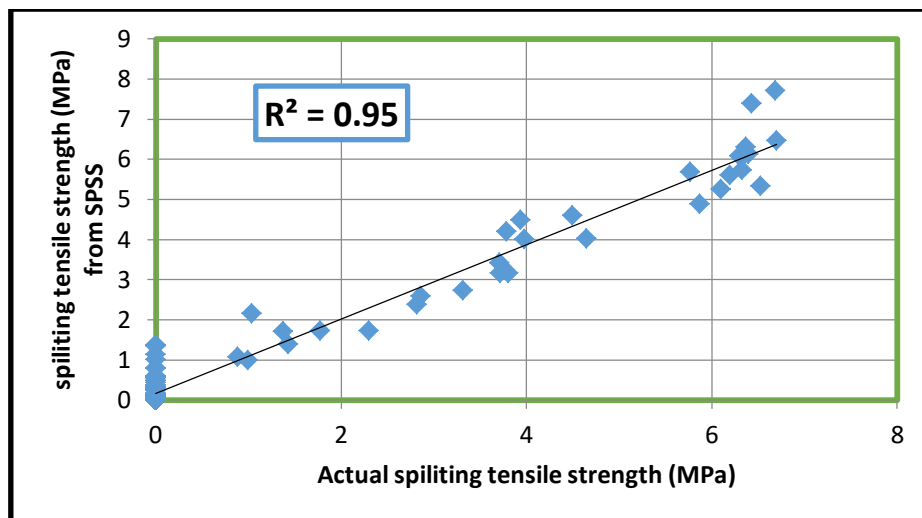
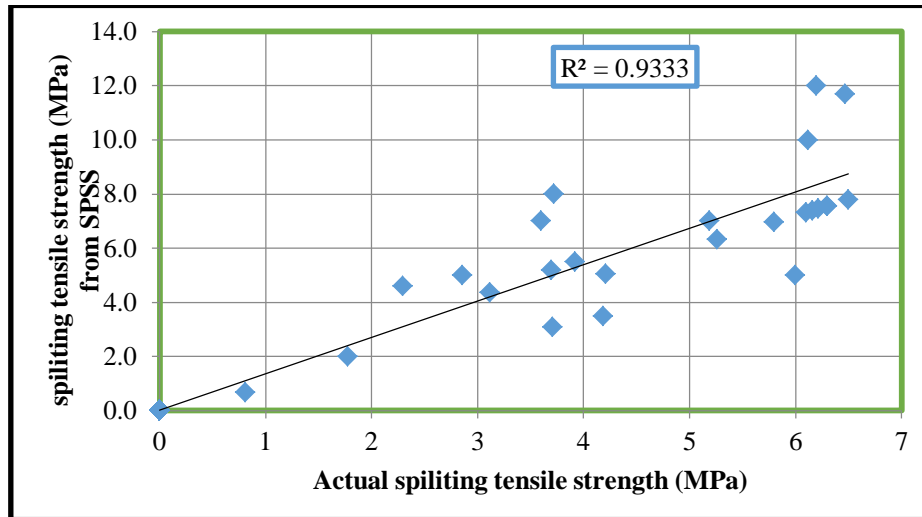
$$\text{Splitting} = 1.037CA + 6.199FA - 5.045FSH + 4.710GGB - 2.163SL - 2.820NH - 7.715NS - 12.209W + 0.420SP$$

- **For 28 curing days**

$$\text{Splitting} = 2.653CA - 1.938FA - 4.703 FSH - 5.969GGB + 3.426NH + 8.659NS + 15.408W + 2.651SP$$

- For 90 curing days

**Splitting=** -3.339CA +3.766FA -4.264FSH +2.439GGB -2.816NH -  
7.097NS -9.497W +3.032 SP



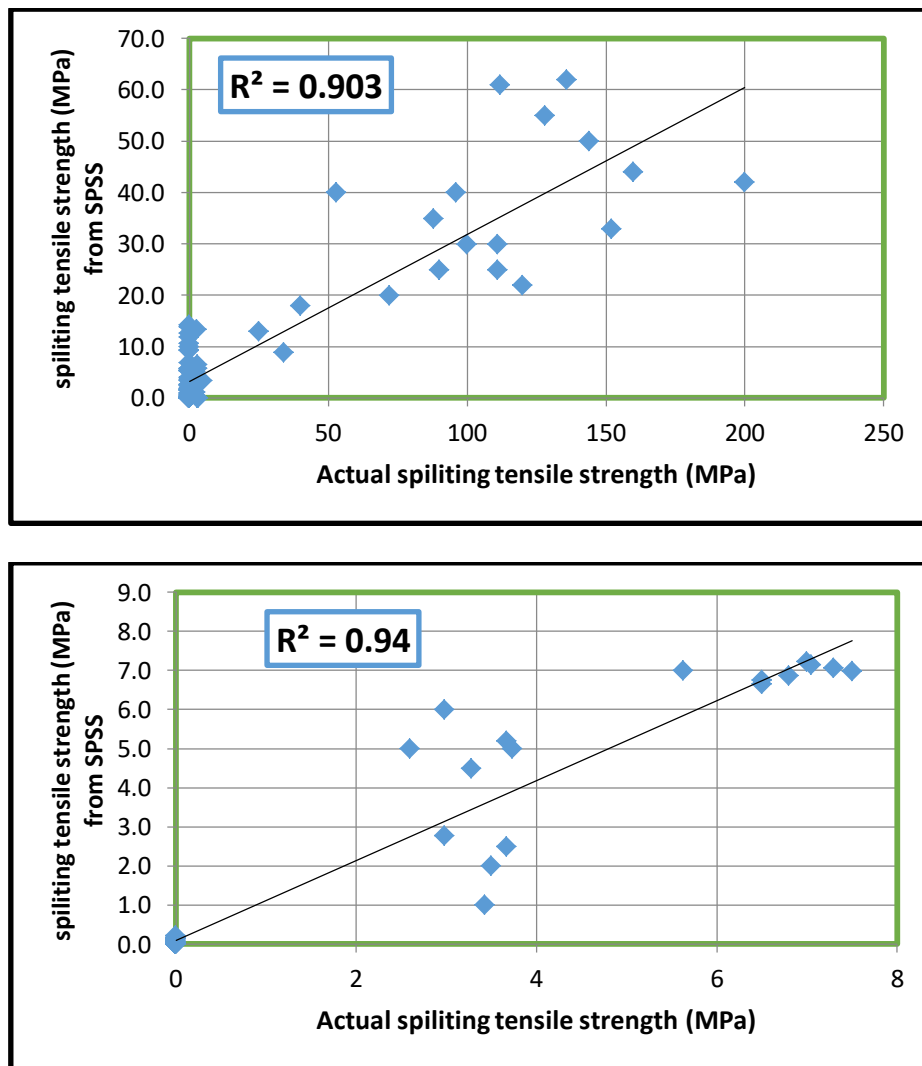


Figure (4.9) Splitting Tensile Strength for Geopolymer concrete by SPSS at 3, 7, 28 and 90 curing days.

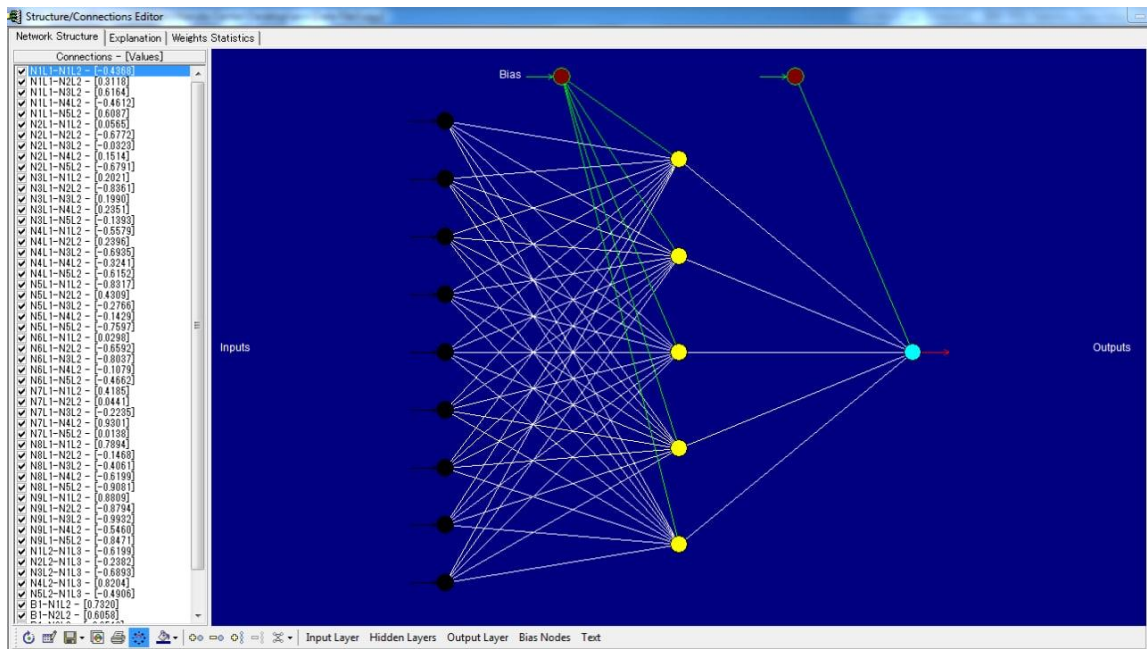
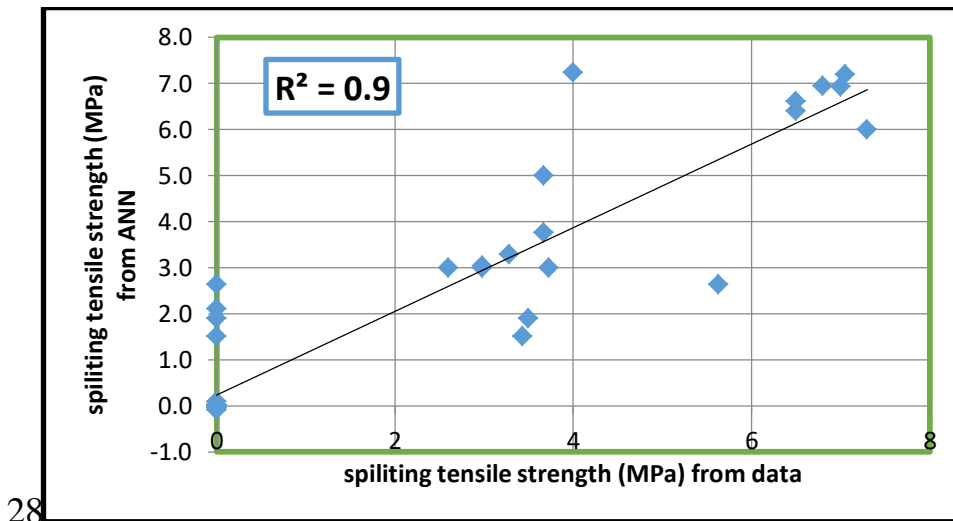
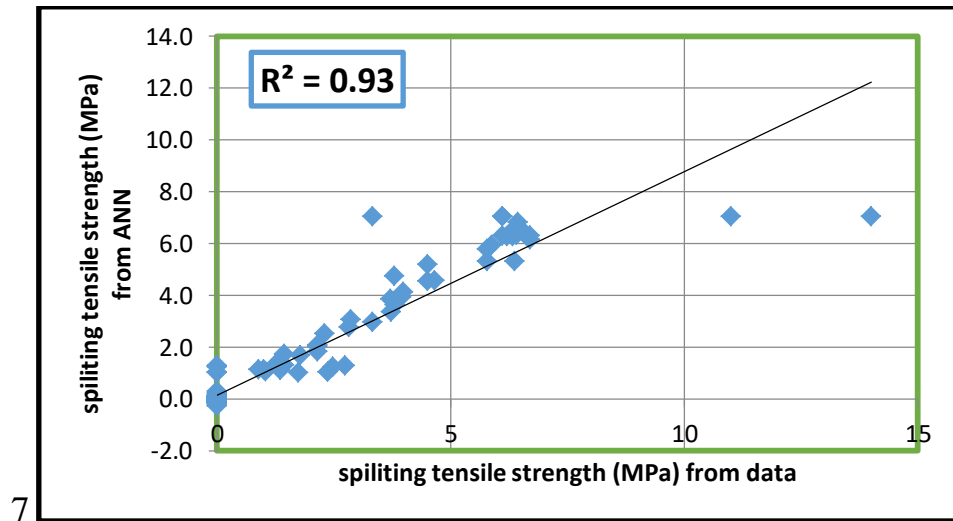
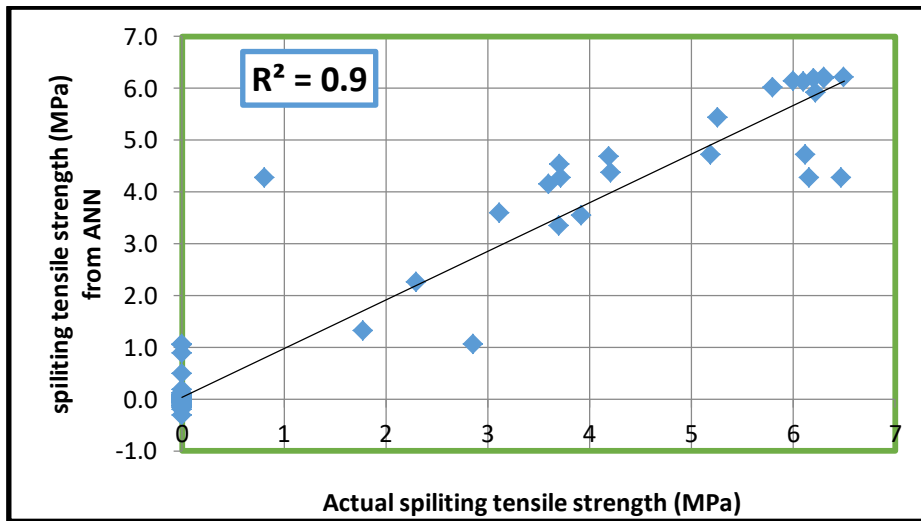


Figure (4.10) ANN structure of Splitting Tensile Strength prediction.

The best ANN connections from the succeeded model are utilized to evolve the forecast models for Splitting Tensile Strength as illustrated in Figure (4.11)



Figure (4.11) ANNs Weight Distribution of the succeeded model for Splitting Tensile Strength.



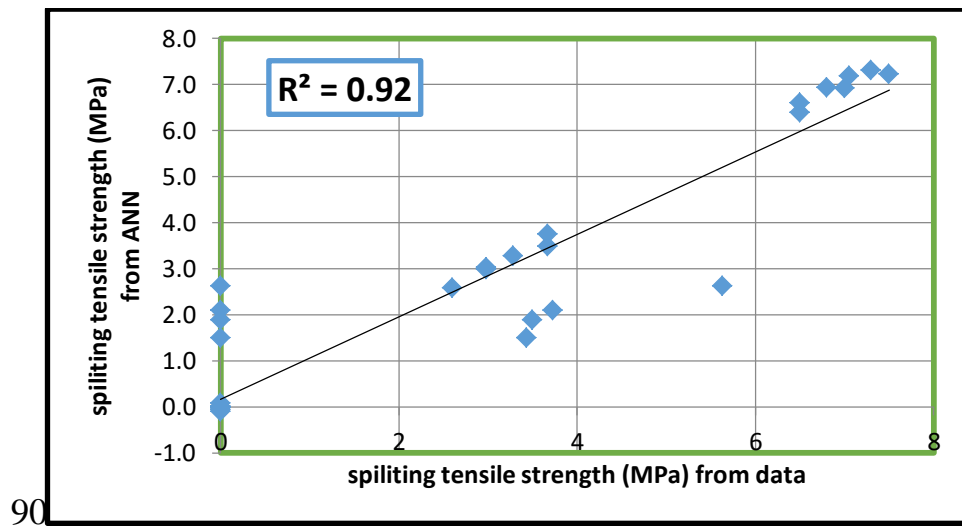


Figure (4.12) Splitting Tensile Strength for Geopolymer concrete by ANN at 3, 7, 28 and 90 curing days.

#### 4.4.3. Flexural Strength

Rupture Modulus is a method of determining the geopolymer concretes' flexural strength by using simple beams/prisms with third-point stress. Geopolymer concretes generally exhibits high compressive strength, limited endurance, and poor flexural quality that might limit its use in auxiliary structures (Roy et al., 2000). Figure (4.13) demonstrate the correlation between the flexural strength from SPSS and flexural strength from data for predicted flexural strength, where the best model expression for the regression coefficient ( $R^2$ ) value was 0.86. Figure (4.16) demonstrate the correlation between the flexural strength from ANN and flexural strength from data for predicted flexural strength, where the best model expression for the regression coefficient ( $R^2$ ) value was 0.914. However, ANN present better regression coefficient comparison with SPSS results.

Predictive models of Flexural, as derived by MRA, are as follows=

- **For 3 curing days**

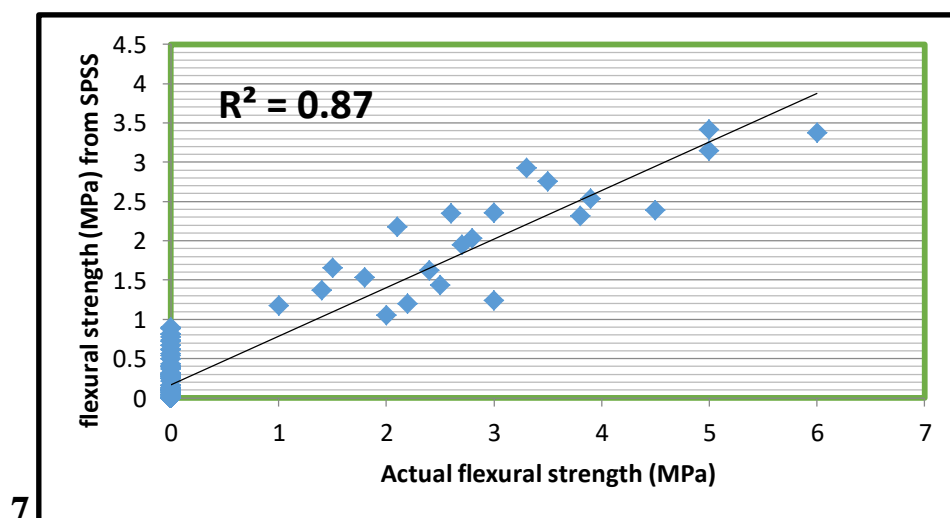
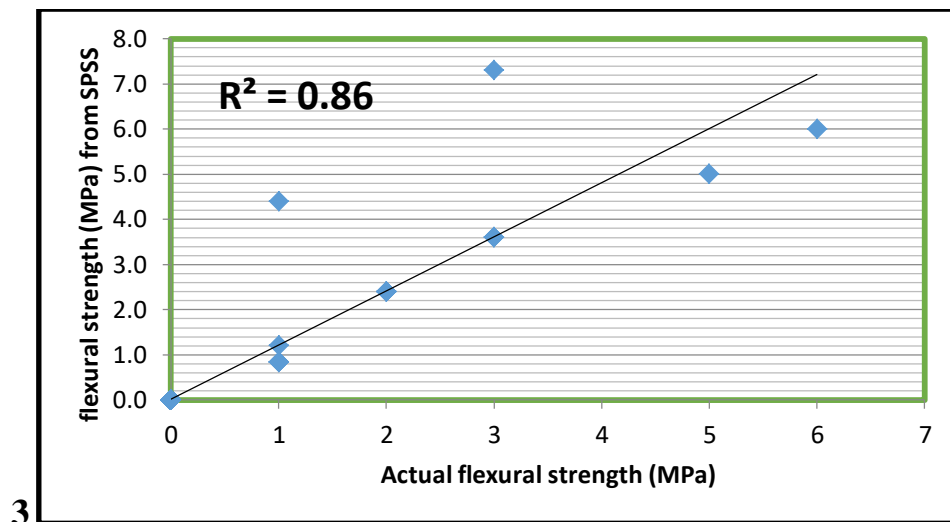
$$\text{FLEXURAL} = -0.758\text{FA} + 0.195\text{FSH} - 1.292\text{GGB} + 0.294\text{SL} + 1.190\text{NS} + 0.727\text{SP}$$

- For 7 curing days

$$\text{FLEXURAL} = -6.001\text{CA} - 6.469\text{FA} - 1.884\text{FSH} - 4.052\text{GGB} - 3.084\text{SL} + 4.33\text{NH} + 8.290\text{NS}$$

- For 28 curing days

$$\text{FLEXURAL} = 2.848\text{CA} + 2.859\text{FA} + 2.754\text{FSH} + 2.757\text{GGB} + 2.696\text{W}$$



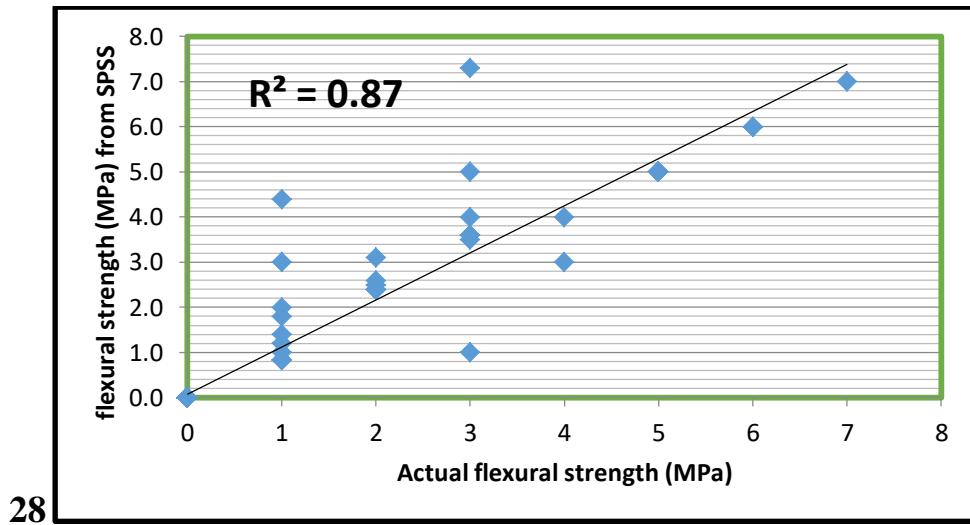


Figure (4.13) Flexural Strength for Geopolymer concrete by SPSS at 3, 7, and 28 curing days.

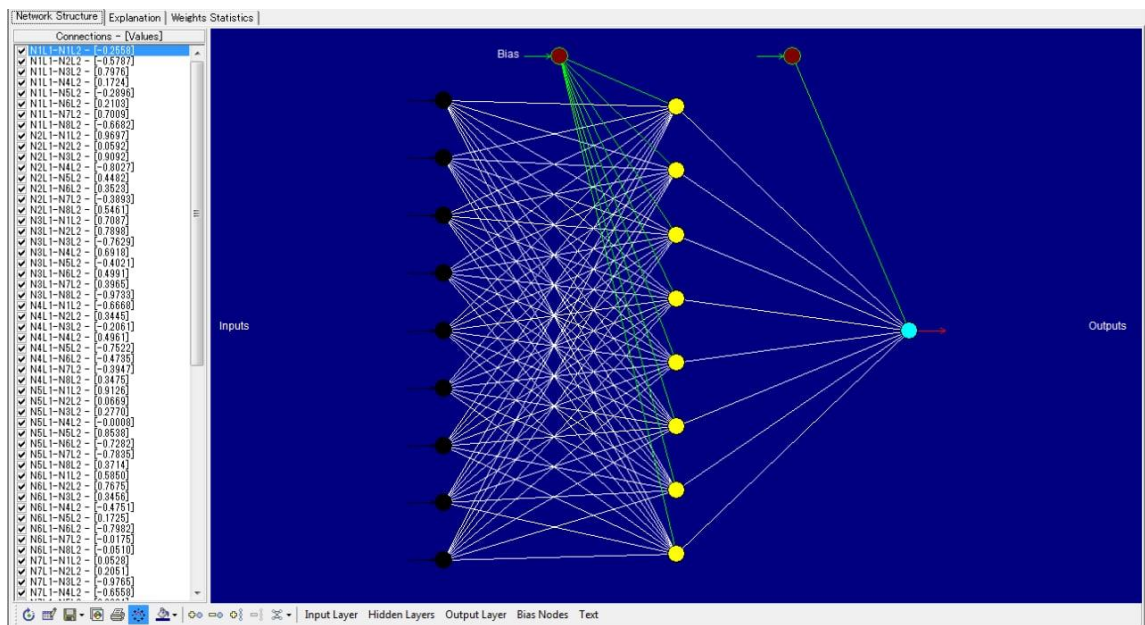


Figure (4.14) ANN structure of Flexural Strength prediction.

The best ANN connections from the succeeded model are utilized to evolve the forecast models for Flexural strength as illustrated in Figure (4.15)

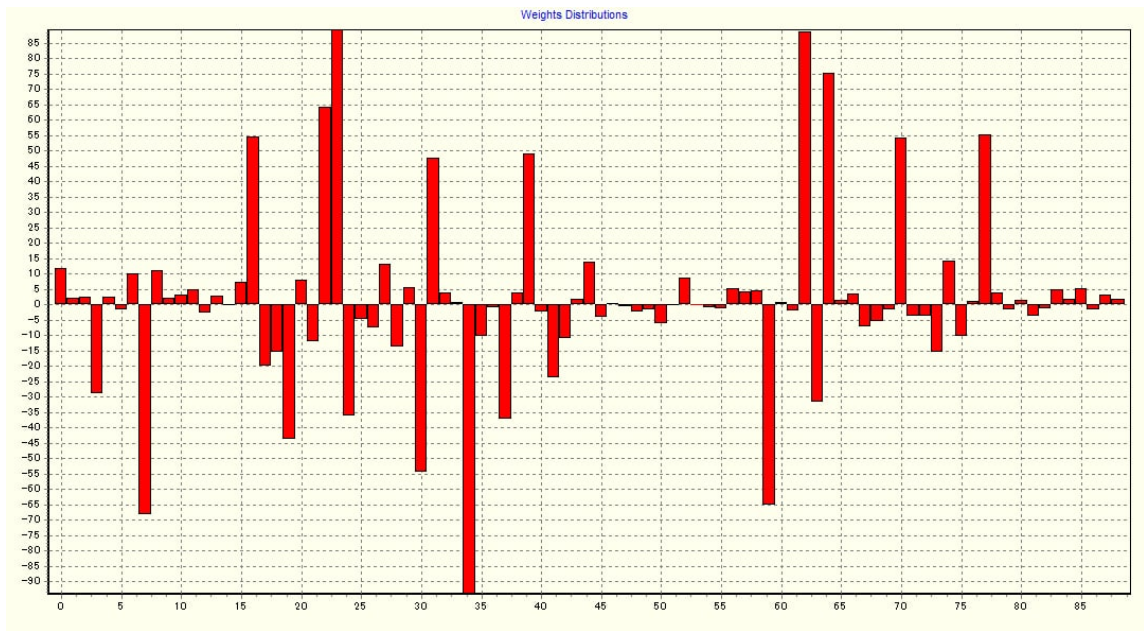
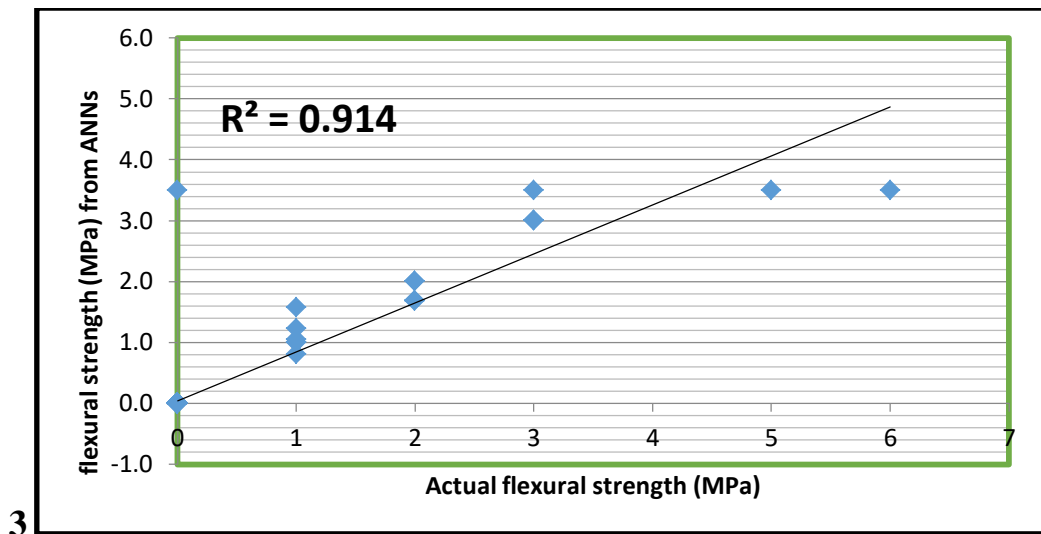


Figure (4.15) ANNs Weight Distribution of the succeeded model for Flexural Strength.



3

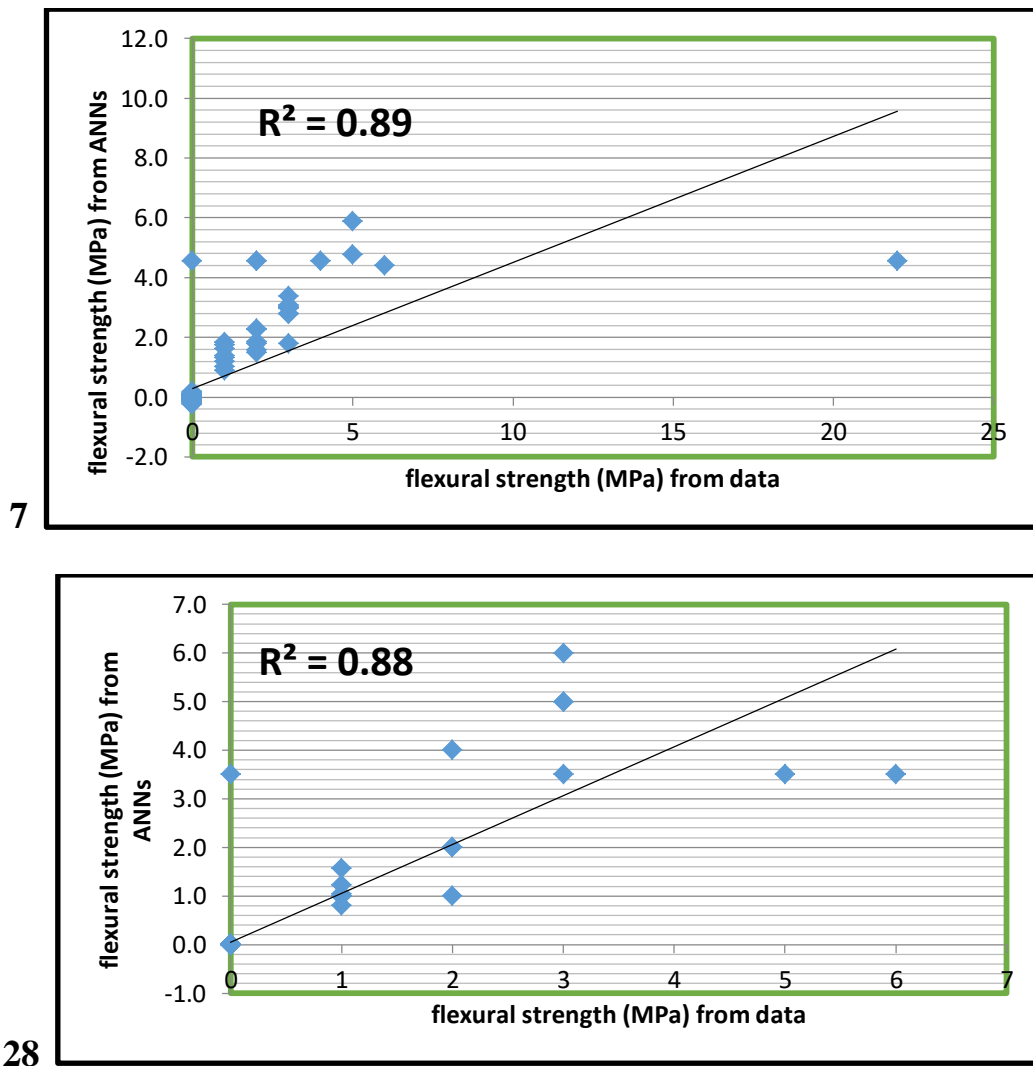


Figure (4.16) Flexural Strength for Geopolymer concrete by ANN at 3, 7, and 28 curing days.

#### 4.4.4. Dry Shrinkage Results

Drying shrinkage is the reduction in volume of concretes or cement over time, irrespective of external processes, resulting in cracking or a reduction in load-carrying capability due to volume loss. Once the sections of a concretes structure are unable to sustain the stress or the repeated cycles of expansion, cracks may form. Previous study has shown that geopolymers outperform standard OPC in terms of expansion and shrinkage resistant (Fernández-Jiménez et al., 2007; Wallah, 2009), as well as thermal

characteristics once subjected to high temperatures (800 to 1000 degree centigrade) (Gilbert, 2002).

Figure (4.17) demonstrate the correlation between the dry shrinkage from SPSS and dry shrinkage from data for predicted dry shrinkage, where the best model expression for the regression coefficient ( $R_2$ ) value was 0.8877. Figure (4.20) demonstrate the correlation between the dry shrinkage from ANN and dry shrinkage from data for predicted dry shrinkage, where the best model expression for the regression coefficient ( $R_2$ ) value was 0.89. However, ANN present better regression coefficient comparison with SPSS results.

Predictive models of Shrinkage, as derived by MRA, are as follows=

- **For 3 curing days**

Shrinkage= 0.211CA +0.061FA +0.306GGB -1.039SL -1.284NH -0.013W - 0.325SP

- **For 7 curing days**

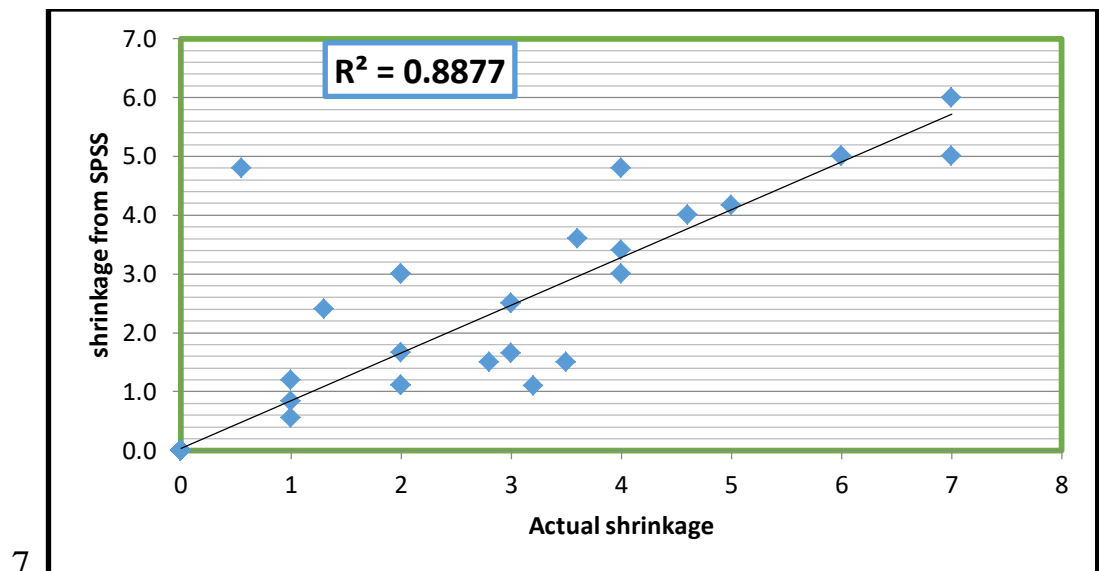
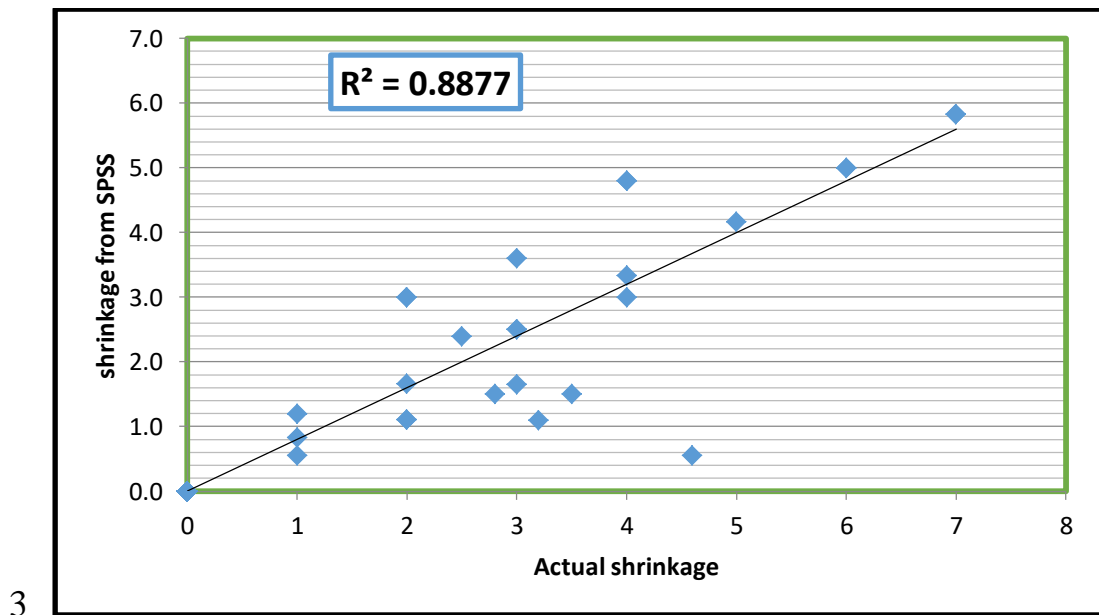
Shrinkage = 16.116CA +22.975FSH -0.113GGB -11.015SL +58.238NH - 32.599NS -4.757W -4.720SP

- **For 28 curing days**

Shrinkage= -1.680GGB -1.423NH -0.277NS +1.147W +0.542SP

- **For 90 curing days**

**SHRINKAGE=** 9.263CA+1.631FA -0.642FSH +2.548GGB -1.394NH +3.472NS -1.229W -9.647SP



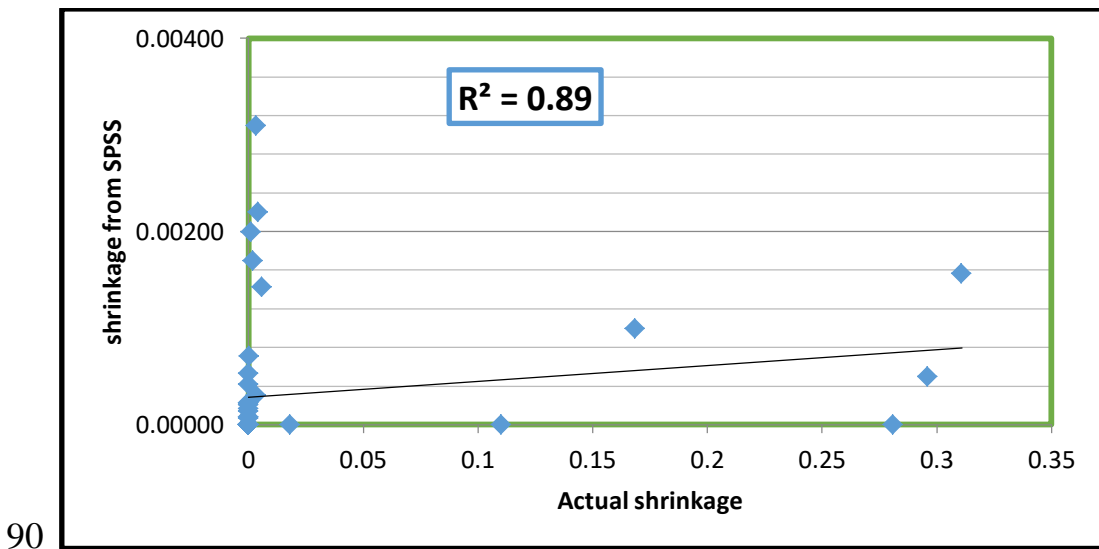
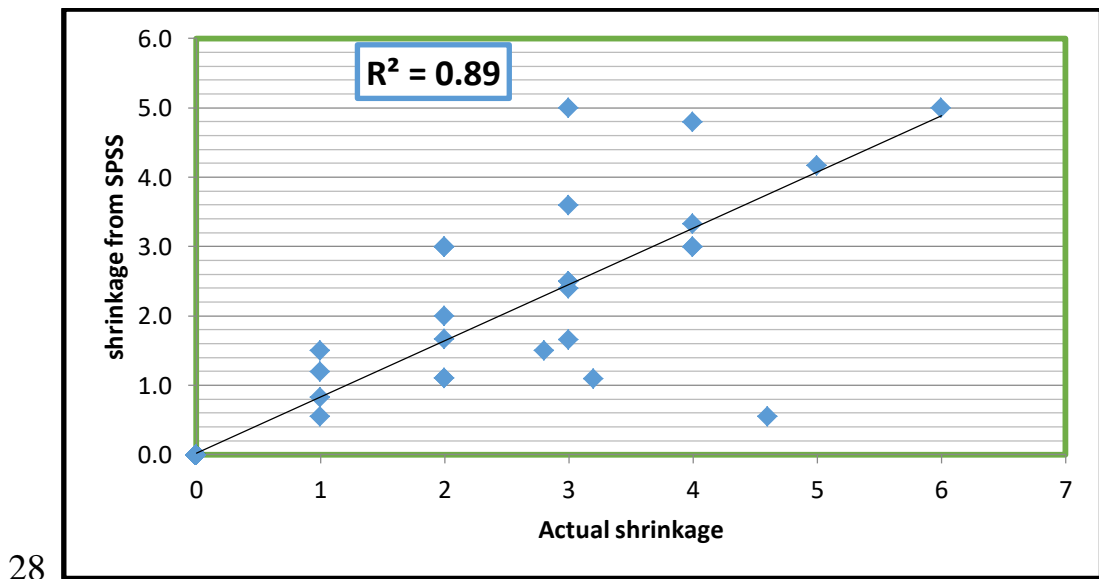


Figure (4.17) Dry Shrinkage results for Geopolymer concrete by SPSS at 3, 7, 28 and 90 curing days.

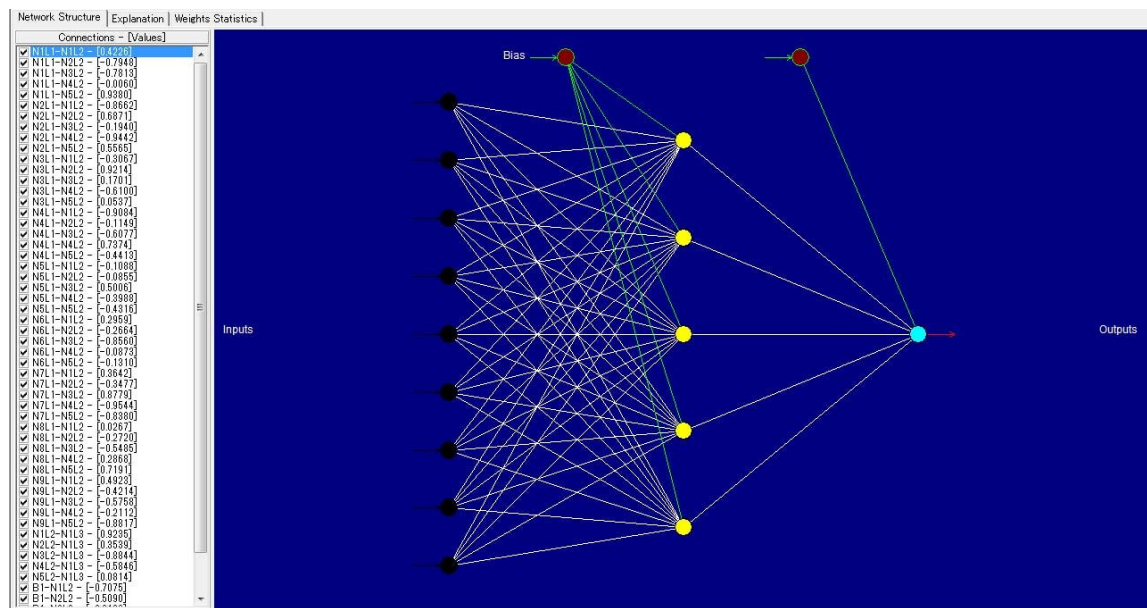


Figure (4.18) ANN structure of dry Shrinkage prediction.

The best ANN connections from the succeeded model are utilized to evolve the forecast models for dry Shrinkage results as illustrated in Figure (4.19)

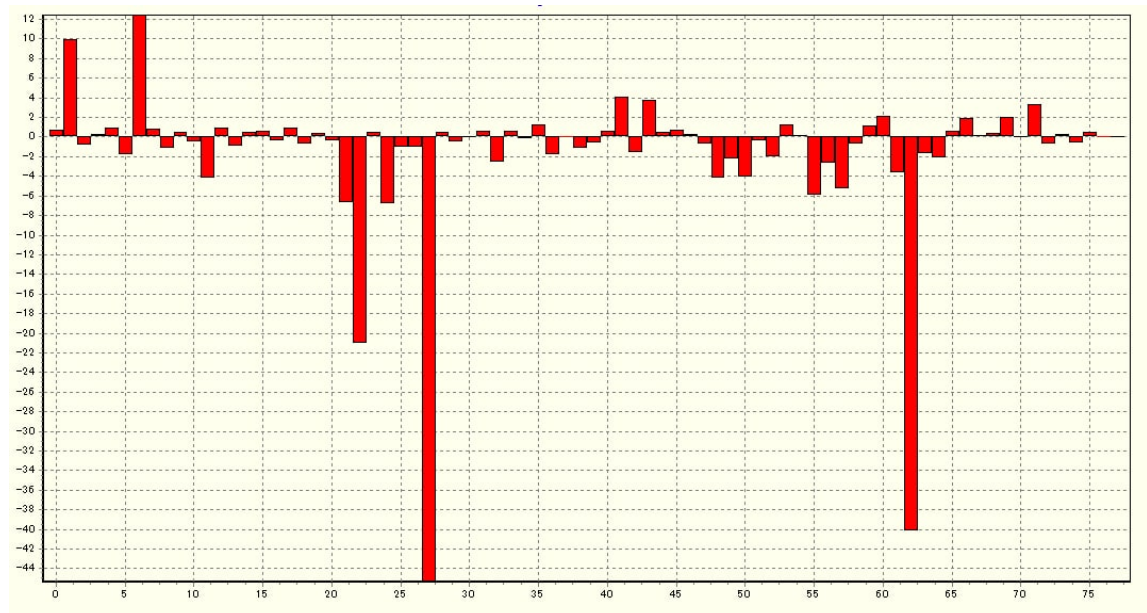


Figure (4.19) ANNs Weight Distribution of the succeeded model for Shrinkage results.



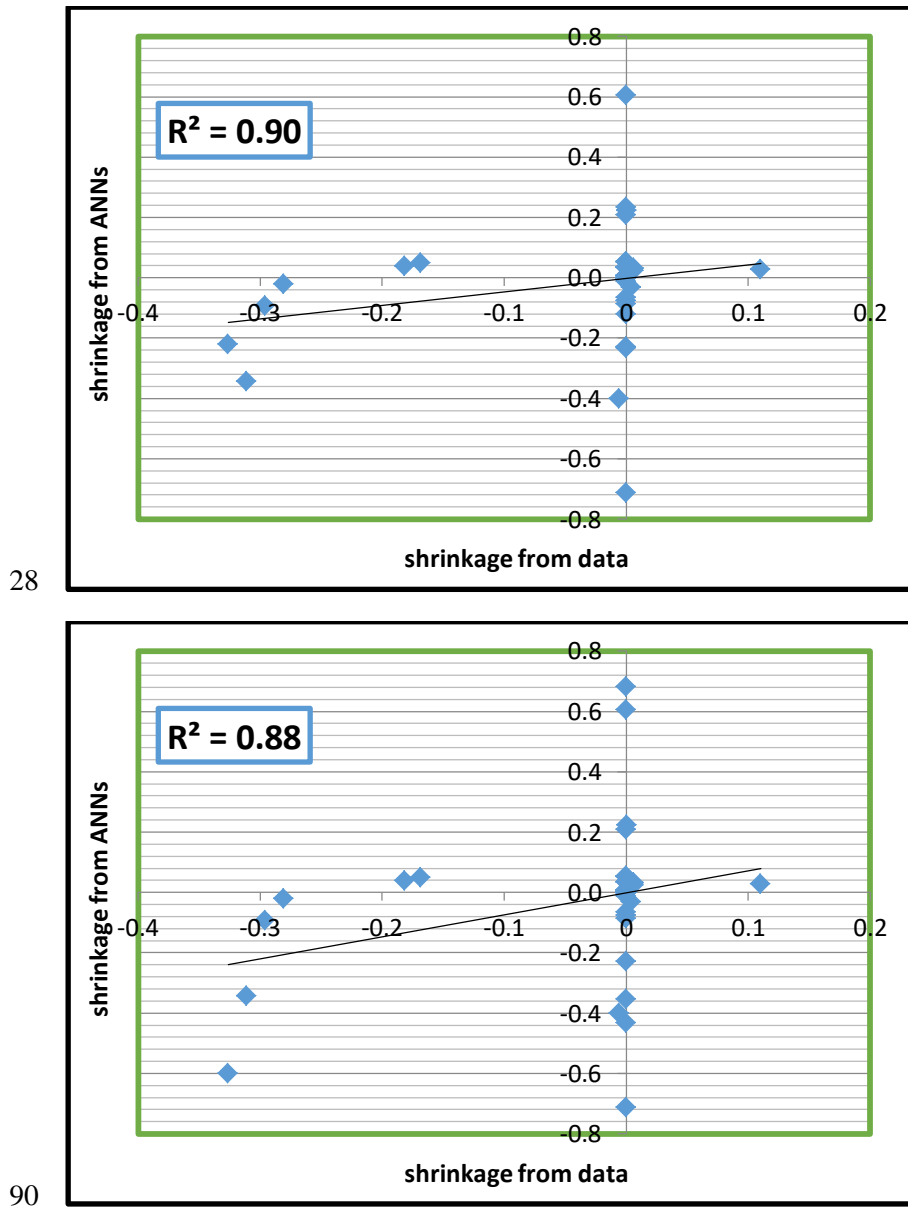


Figure (4.20) Dry Shrinkage results for Geopolymer concrete by ANN at 3, 7, 28 and 90 curing days.

#### 4.4.5. Permeability Results

Sorptivity, permeability, namely absorption, and , water penetrability are key indicators of concretes durability. Permeability via a absorption, diffusion, and porous material all contribute to liquid penetration into concretes. Pores in concretes play a crucial function in allowing liquids and

fluids to pass through the concrete. Nevertheless, the ability of concretes to collect and convey water by capillary forces was influenced by its pore width, tortuosity, continuity, and, distribution, as well as its porosity (Olivia, et al., 2008).

Figure (4.21) demonstrate the correlation between the predicted permeability from SPSS and actual permeability, where the best model expression for the regression coefficient ( $R^2$ ) value was 0.97. Figure (4.22) demonstrate the correlation between the permeability from ANN and actual permeability, where the best model expression for the regression coefficient ( $R_2$ ) value was 0.95. However, SPSS present better regression coefficient comparison with ANN results.

Predictive models of permeability, as derived by MRA, are as follows=

$$\text{PERMEABILITY} = -2.722CA + 2.501FA - 3.615 FSH + 4.523 GGB - 2.043 NH - 4.287 NS - 4.516W + 2.368SP$$

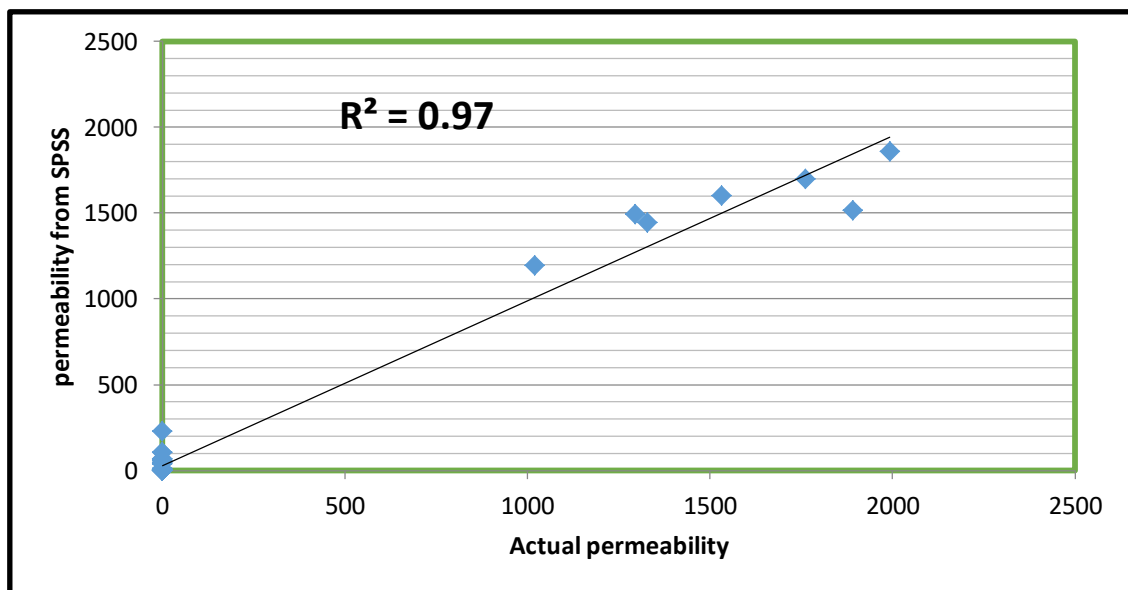


Figure (4.21) Permeability results for Geopolymer concrete by SPSS at 90 curing days.

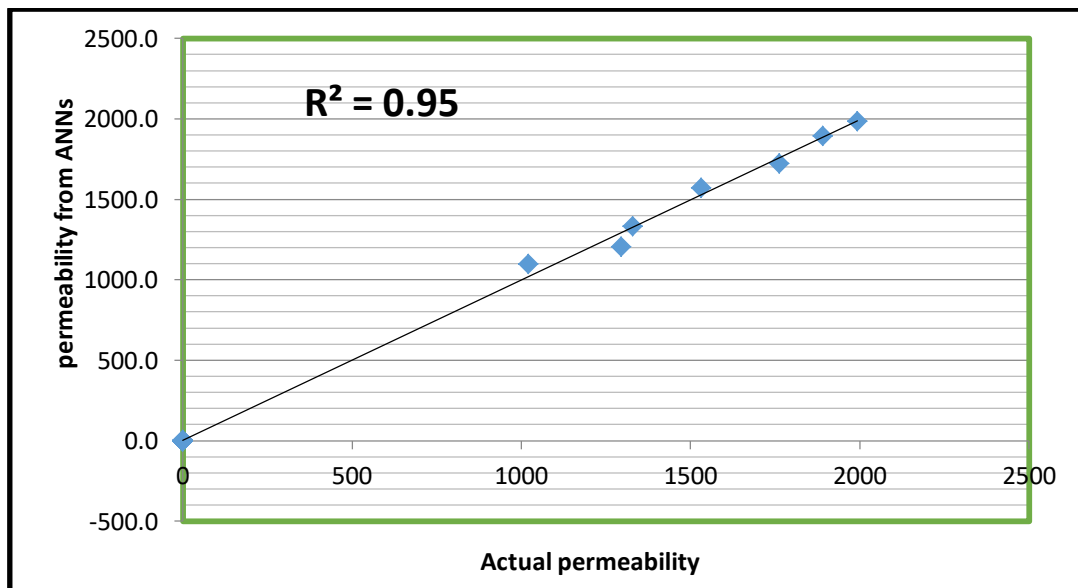


Figure (4.22) Permeability results for Geopolymer concrete by ANN at 90 curing days.

## Chapter Five

### Conclusions and Recommendations

#### 5.1 General

In this chapter, the conclusions of the present study obtained from the statistical results with the limitations of the study. And this chapter was finished with mentioned recommendations for future researchers.

#### 5.2 Conclusions

From the results of the present study, the following conclusions are obtained:

1. The main parameters which influence the compressive strength and fresh properties of Geopolymer concrete are (fly ash, silica fume, GGBS, Metakaolin, rice husk ash, coarse aggregate, fine aggregate, NaOH sol, Na<sub>2</sub>SiO<sub>3</sub> sol, SP and Alkaline activator, w/b).
2. The strength characteristics of Geopolymer concrete (compressive strength, tensile strength, flexural strength and dry shrinkage) data have been obtained at (3, 7, 28, 90) curing days. And the prediction model was created using SPSS and ANN software.
3. The regression coefficient (R<sub>2</sub>) value for compressive strength were 0.94 and 0.9635 using SPSS and ANN, respectively. ANN present better regression coefficient comparison with SPSS results.
4. The regression coefficient (R<sub>2</sub>) value for Splitting Tensile Strength were 0.9333 and 0.9 using SPSS and ANN, respectively. SPSS present better regression coefficient comparison with ANN results.
5. The regression coefficient (R<sub>2</sub>) value for dry shrinkage were 0.8877 and 0.89 using SPSS and ANN, respectively. ANN present better regression coefficient comparison with SPSS results.

6. The regression coefficient ( $R_2$ ) value for flexural strength were 0.86 and 0.914 using SPSS and ANN, respectively. ANN present better regression coefficient comparison with SPSS results.
7. The regression coefficient ( $R_2$ ) value for flexural strength were 0.8778 and 0.92 using SPSS and ANN, respectively. ANN present better regression coefficient comparison with SPSS results.

### 5.3 Recommendations For The Future Works

1. There should be a data bank system for performing compressive tests for Geopolymer concrete, which can serve as a key input to predicate models.
2. It must be taken into consideration the arrangement of variables and their effect on properties of Geopolymer concrete.
3. Beware of using inappropriate variables that could cause results to deviate.
4. It is possible to find new predictive models by using ANN program and compare them with the results of SPSS program.
5. Using different NaOH sol and  $\text{Na}_2\text{SiO}_3$  sol molarity in order to investigated the effect of molarity on the behavior of geopolymer concrete characteristics such as compressive strength and tensile strength.
6. Using data that deals with different curing process such as changing the curing temperatures and the others factors that effect on curing like humidity.

### Reference

- 232, A. C. I. C. (2003). *Use of Fly Ash in Concrete. ACI 232.2-03*.
- Abdullah, M. M. A. B., Hussin, K., Bnhussain, M., Ismail, K. N., Yahya, Z., & Abdul Razak, R. (2012). Fly ash-based geopolymer lightweight concrete using foaming agent. *International Journal of Molecular Sciences*, *13*(6), 7186–7198.
- Abdullah, M. M. A. B., Kamarudin, H., Bnhussain, M., Khairul Nizar, I., Rafiza, A. R., & Zarina, Y. (2011). The relationship of NaOH molarity, Na<sub>2</sub>SiO<sub>3</sub>/NaOH ratio, fly ash/alkaline activator ratio, and curing temperature to the strength of fly ash-based geopolymer. *Advanced Materials Research*, *328*, 1475–1482.
- Adam, A. A., & Horianto, X. X. X. (2014). The effect of temperature and duration of curing on the strength of fly ash based geopolymer mortar. *Procedia Engineering*, *95*, 410–414.
- Akkurt, S., Tayfur, G., & Can, S. (2004). Fuzzy logic model for the prediction of cement compressive strength. *Cement and Concrete Research*, *34*(8), 1429–1433.
- Alaneme George, U., & Mbadike Elvis, M. (2019). Modelling of the mechanical properties of concrete with cement ratio partially replaced by aluminium waste and sawdust ash using artificial neural network. *SN Applied Sciences*, *1*(11), 1–18.
- Alireza, N. G., Suraya, A. R., Farah, N. A. A., & Mohamad, A. M. S. (2010). Experimental investigation of the size effects of \$ SiO\_2 \$ nano-particles on the mechanical properties of binary bended cement. *Compos. Part B Eng*, *41*, 673–677.
- Almuhsin, B., al-Attar, T., & Hasan, Q. (2018). Effect of discontinuous

## Reference

---

- curing and ambient temperature on the compressive strength development of fly ash based Geopolymer concrete. *MATEC Web of Conferences*, 162, 2026.
- Anıl, N. İ. Ş. (2019). Compressive strength variation of alkali activated fly ash/slag concrete with different NaOH concentrations and sodium silicate to sodium hydroxide ratios. *Journal of Sustainable Construction Materials and Technologies*, 4(2), 351–360.
- Assi, L. N., Deaver, E. E., ElBatanouny, M. K., & Ziehl, P. (2016). Investigation of early compressive strength of fly ash-based geopolymer concrete. *Construction and Building Materials*, 112, 807–815.
- Bondar, D., Lynsdale, C. J., Milestone, N. B., Hassani, N., & Ramezaniyanpour, A. A. (2011). Engineering properties of alkali-activated natural pozzolan concrete. *ACI Materials Journal*, 108(1), 64–72.
- Chi, M. (2017). Effects of the alkaline solution/binder ratio and curing condition on the mechanical properties of alkali-activated fly ash mortars. *Science and Engineering of Composite Materials*, 24(5), 773–782.
- Chindapasirt, P., Chareerat, T., & Sirivivatnanon, V. (2007). Workability and strength of coarse high calcium fly ash geopolymer. *Cement and Concrete Composites*, 29(3), 224–229.
- Chindapasirt, P., & Ridtirud, C. (2020). High calcium fly ash geopolymer containing natural rubber latex as additive. *GEOMATE Journal*, 18(69), 124–129.
- Chithambaram, S. J., Kumar, S., Prasad, M. M., & Adak, D. (2018). Effect of parameters on the compressive strength of fly ash based geopolymer

## Reference

---

- concrete. *Structural Concrete*, 19(4), 1202–1209.
- Collins, F., & Sanjayan, J. (2002). Development of novel alkali activated slag binders to achieve high early strength concrete for construction use. *Australian Civil Engineering Transactions*, 44, 91–102.
- Criado, M., Palomo, A., & Fernández-Jiménez, A. (2005). Alkali activation of fly ashes. Part 1: Effect of curing conditions on the carbonation of the reaction products. *Fuel*, 84(16), 2048–2054.
- Cross, D., Stephens, J., & Vollmer, J. (2005). Field trials of 100% fly ash concrete. *Concrete International*, 27(9), 47–51.
- Davidovits, J. (1991). Geopolymers: inorganic polymeric new materials. *Journal of Thermal Analysis and Calorimetry*, 37(8), 1633–1656.
- Davidovits, J., Buzzi, L., Rocher, P., Gimeno, D., Marini, C., & Tocco, S. (1999). Geopolymeric cement based on low cost geologic materials. Results from the european research project geocistem. *Proceedings of the 2nd International Conference on Geopolymer*, 99, 83–96.
- Davidovits, J., & Davidovics, M. (1991). Geopolymer: ultra-high temperature tooling material for the manufacture of advanced composites. *How Concept Becomes Reality.*, 36, 1939–1949.
- De Vargas, A. S., Dal Molin, D. C. C., Vilela, A. C. F., Da Silva, F. J., Pavao, B., & Veit, H. (2011). The effects of Na<sub>2</sub>O/SiO<sub>2</sub> molar ratio, curing temperature and age on compressive strength, morphology and microstructure of alkali-activated fly ash-based geopolymers. *Cement and Concrete Composites*, 33(6), 653–660.
- Djwantoro, H., Wallah, S. E., Sumajouw, M. J. D., & Rangan, B. V. (2004). On the development of fly ash-based geopolymer concrete. *ACI Materials Journal*, 101(6), 467–472.

## Reference

---

- Duxson, Peter, Fernández-Jiménez, A., Provis, J. L., Lukey, G. C., Palomo, A., & van Deventer, J. S. J. (2007). Geopolymer technology: the current state of the art. *Journal of Materials Science*, *42*(9), 2917–2933.
- Duxson, PSWM, Mallicoat, S. W., Lukey, G. C., Kriven, W. M., & van Deventer, J. S. J. (2007). The effect of alkali and Si/Al ratio on the development of mechanical properties of metakaolin-based geopolymers. *Colloids and Surfaces A: Physicochemical and Engineering Aspects*, *292*(1), 8–20.
- Falah, M., Obenaus-Emler, R., Kinnunen, P., & Illikainen, M. (2020). Effects of Activator Properties and Curing Conditions on Alkali-Activation of Low-Alumina Mine Tailings. *Waste and Biomass Valorization*, *11*(9), 5027–5039. <https://doi.org/10.1007/s12649-019-00781-z>
- Fang, G., Ho, W. K., Tu, W., & Zhang, M. (2018). Workability and mechanical properties of alkali-activated fly ash-slag concrete cured at ambient temperature. *Construction and Building Materials*, *172*, 476–487.
- Fernández-Jiménez, A., García-Lodeiro, I., & Palomo, A. (2007). Durability of alkali-activated fly ash cementitious materials. *Journal of Materials Science*, *42*(9), 3055–3065.
- Gençel, O., Karadag, O., Oren, O. H., & Bilir, T. (2021). Steel slag and its applications in cement and concrete technology: A review. *Construction and Building Materials*, *283*, 122783.
- Gilbert, R. I. (2002). Creep and shrinkage models for high strength concrete—Proposals for inclusion in AS3600. *Australian Journal of Structural Engineering*, *4*(2), 95–106.
- Golafshani, E. M., Behnood, A., & Arashpour, M. (2020). Predicting the

## Reference

---

- compressive strength of normal and High-Performance Concretes using ANN and ANFIS hybridized with Grey Wolf Optimizer. *Construction and Building Materials*, 232, 117266.
- Görhan, G., & Kürklü, G. (2014). The influence of the NaOH solution on the properties of the fly ash-based geopolymer mortar cured at different temperatures. *Composites Part b: Engineering*, 58, 371–377.
- Guo, X., Shi, H., & Dick, W. A. (2010). Compressive strength and microstructural characteristics of class C fly ash geopolymer. *Cement and Concrete Composites*, 32(2), 142–147.
- Haji-Esmaelii, H. (2012). *Admixtures for use in geopolymers*.
- Harrison, A. J. W., & FCPA, B. S. B. E. (n.d.). *Towards Making Pre-Mix Concrete Foolproof*.
- Hassan, A., Arif, M., & Shariq, M. (2019). Effect of curing condition on the mechanical properties of fly ash-based geopolymer concrete. *SN Applied Sciences*, 1(12), 1–9.
- He, J., Jie, Y., Zhang, J., Yu, Y., & Zhang, G. (2013). Synthesis and characterization of red mud and rice husk ash-based geopolymer composites. *Cement and Concrete Composites*, 37, 108–118.
- Jawahar, J. G., & Mounika, G. (2016). Strength properties of fly ash and GGBS based geopolymer concrete. *Asian J. Civ. Eng.(BHRC)*, 17(1), 127–135.
- Jindal, B. B. (2019). Investigations on the properties of geopolymer mortar and concrete with mineral admixtures: A review. *Construction and Building Materials*, 227, 116644.
- Jindal, B. B., Parveen, Singhal, D., & Goyal, A. (2017). Predicting relationship between mechanical properties of low calcium fly ash-

## Reference

---

- based geopolymer concrete. *Transactions of the Indian Ceramic Society*, 76(4), 258–265.
- Joseph, B., & Mathew, G. (2012). Influence of aggregate content on the behavior of fly ash based geopolymer concrete. *Scientia Iranica*, 19(5), 1188–1194.
- Junaid, M. T., Elbana, A., & Altoubat, S. (2020). Flexural response of geopolymer and fiber reinforced geopolymer concrete beams reinforced with GFRP bars and strengthened using CFRP sheets. *Structures*, 24, 666–677.
- Khale, D., & Chaudhary, R. (2007). Mechanism of geopolymerization and factors influencing its development: a review. *Journal of Materials Science*, 42(3), 729–746.
- Kumar, V. S., Ganesan, N., & Indira, P. V. (2017). Effect of molarity of sodium hydroxide and curing method on the compressive strength of ternary blend geopolymer concrete. *IOP Conference Series: Earth and Environmental Science*, 80(1), 12011.
- Kurtoglu, A. E., Alzebaree, R., Aljumaili, O., Nis, A., Gulsan, M. E., Humur, G., & Cevik, A. (2018). Mechanical and durability properties of fly ash and slag based geopolymer concrete. *Advances in Concrete Construction*, 6(4), 345.
- Lee, N. K., Jang, J. G., & Lee, H.-K. (2014). Shrinkage characteristics of alkali-activated fly ash/slag paste and mortar at early ages. *Cement and Concrete Composites*, 53, 239–248.
- Lloyd, N., & Rangan, V. (2009). Geopolymer concrete-sustainable cementless concrete. *Proceedings of Tenth ACI International Conference*, 33–53.

## Reference

---

- Mahasenan, N., Smith, S., & Humphreys, K. (2003). The cement industry and global climate change: current and potential future cement industry CO<sub>2</sub> emissions. *Greenhouse Gas Control Technologies-6th International Conference*, 995–1000.
- Masoule, M. S. T., Bahrami, N., Karimzadeh, M., Mohasanati, B., Shoaie, P., Ameri, F., & Ozbakkaloglu, T. (2022). Lightweight geopolymer concrete: A critical review on the feasibility, mixture design, durability properties and microstructure. *Ceramics International*.
- Mehdipour, V., Stevenson, D. S., Memarianfard, M., & Sihag, P. (2018). Comparing different methods for statistical modeling of particulate matter in Tehran, Iran. *Air Quality, Atmosphere & Health*, 11(10), 1155–1165.
- Mejeoumov, G. G. (2007). *Improved cement quality and grinding efficiency by means of closed mill circuit modeling*. Texas A&M University.
- Memon, F. A., Nuruddin, M. F., & Shafiq, N. (2013). Effect of silica fume on the fresh and hardened properties of fly ash-based self-compacting geopolymer concrete. *International Journal of Minerals, Metallurgy, and Materials*, 20(2), 205–213.
- Mohammed, B. S., & Fang, O. C. (2011). Mechanical and durability properties of concretes containing paper-mill residuals and fly ash. *Construction and Building Materials*, 25(2), 717–725.
- Mustafa Al Bakri, A. M., Kamarudin, H., Bnhussain, M., Rafiza, A. R., & Zarina, Y. (2012). Effect of Na<sub>2</sub>SiO<sub>3</sub>/NaOH Ratios and NaOH Molarities on Compressive Strength of Fly-Ash-Based Geopolymer. *ACI Materials Journal*, 109(5).
- Nath, P., & Sarker, P. K. (2017). Flexural strength and modulus of elasticity of ambient-cured blended low-calcium fly ash geopolymer concrete.

## Reference

---

- Construction and Building Materials*, 130, 22–31.
- Neupane, K., Chalmers, D., & Kidd, P. (2018). High-strength geopolymer concrete-properties, advantages and challenges. *Advances in Materials*, 7(2), 15–25.
- Neville, A. M. (2000). *Properties of Concrete. Fourth and Final Version*. Prentice Hall.
- Nguyen, T. T., Goodier, C. I., & Austin, S. A. (2020). Factors affecting the slump and strength development of geopolymer concrete. *Construction and Building Materials*, 261, 119945.
- Nikoloutsopoulos, N., Sotiropoulou, A., Kakali, G., & Tsivilis, S. (2021). Physical and Mechanical Properties of Fly Ash Based Geopolymer Concrete Compared to Conventional Concrete. *Buildings*, 11(5), 178.
- Oderji, S. Y., Chen, B., Ahmad, M. R., & Shah, S. F. A. (2019). Fresh and hardened properties of one-part fly ash-based geopolymer binders cured at room temperature: Effect of slag and alkali activators. *Journal of Cleaner Production*, 225, 1–10.
- Okoye, F. N., Durgaprasad, J., & Singh, N. B. (2016). Effect of silica fume on the mechanical properties of fly ash based-geopolymer concrete. *Ceramics International*, 42(2), 3000–3006.
- Olivia, M., Sarker, P., Nikraz, H. (2008). *Water Penetrability of low calcium fly ash geopolymer concrete. Proc. ICCBT2008-A 46, . June*, 517–530.
- Olivia, M., Tambunan, L. M., & Saputra, E. (2017). Properties of Palm Oil Fuel Ash (POFA) Geopolymer Mortar Cured at Ambient Temperature. *MATEC Web of Conferences*, 97, 1006.
- Oyebisi, S., Ede, A., Olutoge, F., & Omole, D. (2020). Geopolymer

## Reference

---

- concrete incorporating agro-industrial wastes: Effects on mechanical properties, microstructural behaviour and mineralogical phases. *Construction and Building Materials*, 256, 119390.
- Partha, S. D., Pradip, N., & Prabir, K. S. (2013). Strength and permeation properties of slag blended fly ash based geopolymer concrete. *Advanced Materials Research*, 651, 168–173.
- Parveen, A., Liu, W., Hussain, S., Asghar, J., Perveen, S., & Xiong, Y. (2019). Silicon priming regulates morpho-physiological growth and oxidative metabolism in maize under drought stress. *Plants*, 8(10), 431.
- Phoo-Ngernkham, T., Phiangphimai, C., Damrongwiriyanupap, N., Hanjitsuwan, S., Thumrongvut, J., & Chindaprasirt, P. (2018). A mix design procedure for alkali-activated high-calcium fly ash concrete cured at ambient temperature. *Advances in Materials Science and Engineering*, 2018.
- Posi, P., Teerachanwit, C., Tanutong, C., Limkamoltip, S., Lertnimoolchai, S., Sata, V., & Chindaprasirt, P. (2013). Lightweight geopolymer concrete containing aggregate from recycle lightweight block. *Materials & Design (1980-2015)*, 52, 580–586.
- Prakasam, G., Murthy, A. R., & Saffiq Rehemani, M. (2020). Mechanical, durability and fracture properties of nano-modified FA/GGBS geopolymer mortar. *Magazine of Concrete Research*, 72(4), 207–216. <https://doi.org/10.1680/jmacr.18.00059>
- Premkumar, R., Chokkalingam, R. B., & Shanmugasundaram, M. (2019). Durability Performance of Fly Ash and Steatite Powder Based Geopolymer Concrete. *IOP Conference Series: Materials Science and Engineering*, 561(1), 12055.
- Premkumar, R., Chokkalingam, R. B., Shanmugasundaram, M., &

## Reference

---

- Ragasree, A. (2020). Study on mechanical properties of alkali activated binary blended binder containing steatite powder and fly ash/GGBS. *IOP Conference Series: Materials Science and Engineering*, 872(1), 12153.
- Provis, J. L., Palomo, A., & Shi, C. (2015). Advances in understanding alkali-activated materials. *Cement and Concrete Research*, 78, 110–125.
- Rajiwala, D. B., & Patil, H. S. (2010). Geopolymer concrete A green concrete. *2010 2nd International Conference on Chemical, Biological and Environmental Engineering*, 202–206.
- Rajini, B., Rao, A. V., & Sashidhar, C. (2020). Cost analysis of geopolymer concrete over conventional concrete. *International Journal of Civil Engineering and Technology*, 11(02).
- Rangan, B. V., Hardjito, D., Wallah, S. E., & Sumajouw, D. M. J. (2005). Studies on fly ash-based geopolymer concrete. *Proceedings of the World Congress Geopolymer, Saint Quentin, France*, 28, 133–137.
- Raut, U., Shalini, A., & Prabu, B. (2019). Strength of geopolymer concrete reinforced with basalt fiber. *Int. Res. J. Eng. Technol*, 6, 3811–3817.
- Reddy, M. S., Dinakar, P., & Rao, B. H. (2016). A review of the influence of source material's oxide composition on the compressive strength of geopolymer concrete. *Microporous and Mesoporous Materials*, 234, 12–23.
- Roy, D. M., Jiang, W., & Silsbee, M. R. (2000). Chloride diffusion in ordinary, blended, and alkali-activated cement pastes and its relation to other properties. *Cement and Concrete Research*, 30(12), 1879–1884.
- Ryu, G. S., Lee, Y. B., Koh, K. T., & Chung, Y. S. (2013). The mechanical

## Reference

---

- properties of fly ash-based geopolymer concrete with alkaline activators. *Construction and Building Materials*, 47, 409–418.
- Saini, G., & Vattipalli, U. (2020). Assessing properties of alkali activated GGBS based self-compacting geopolymer concrete using nano-silica. *Case Studies in Construction Materials*, 12, e00352.
- Samantasinghar, S., & Singh, S. P. (2019). Fresh and hardened properties of fly ash–slag blended geopolymer paste and mortar. *International Journal of Concrete Structures and Materials*, 13(1), 1–12.
- Saravanan, S., & Elavenil, S. (2018). Strength Properties of Geopolymer Concrete using M Sand by Assessing their Mechanical Characteristics. *ARPJ. Eng. Appl. Sci*, 13, 4028–4041.
- Sarker, P. K. (2011). Bond strength of reinforcing steel embedded in fly ash-based geopolymer concrete. *Materials and Structures*, 44(5), 1021–1030.
- Shahmansouri, A. A., Bengar, H. A., & Ghanbari, S. (2020). Compressive strength prediction of eco-efficient GGBS-based geopolymer concrete using GEP method. *Journal of Building Engineering*, 31, 101326.
- Shehab, H. K., Eisa, A. S., & Wahba, A. M. (2016). Mechanical properties of fly ash based geopolymer concrete with full and partial cement replacement. *Construction and Building Materials*, 126, 560–565.
- Shin, S.-K., Um, N., Kim, Y.-J., Cho, N.-H., & Jeon, T.-W. (2020). New policy framework with plastic waste control plan for effective plastic waste management. *Sustainability*, 12(15), 6049.
- Siddique, R., Aggarwal, P., & Aggarwal, Y. (2011). Prediction of compressive strength of self-compacting concrete containing bottom ash using artificial neural networks. *Advances in Engineering Software*,

## Reference

---

- 42(10), 780–786.
- Singhal, D., Junaid, M. T., Jindal, B. B., & Mehta, A. (2018). Mechanical and microstructural properties of fly ash based geopolymer concrete incorporating alccofine at ambient curing. *Construction and Building Materials, 180*, 298–307.
- Sofi, M., Van Deventer, J. S. J., Mendis, P. A., & Lukey, G. C. (2007). Engineering properties of inorganic polymer concretes (IPCs). *Cement and Concrete Research, 37*(2), 251–257.
- Topark-Ngarm, P., Chindaprasirt, P., & Sata, V. (2015). Setting time, strength, and bond of high-calcium fly ash geopolymer concrete. *Journal of Materials in Civil Engineering, 27*(7), 4014198.
- Umniati, B. S., Risdanareni, P., & Zein, F. T. Z. (2017). Workability enhancement of geopolymer concrete through the use of retarder. *AIP Conference Proceedings, 1887*(September).  
<https://doi.org/10.1063/1.5003516>
- Ushaa, T. G., Anuradha, R., & Venkatasubramani, G. S. (2015). *Performance of self-compacting geopolymer concrete containing different mineral admixtures.*
- Van Chanh, N., Trung, B. D., & Van Tuan, D. (2008). Recent research geopolymer concrete. *The 3rd ACF International Conference-ACF/VCA, Vietnam, 18*, 235–241.
- Vijai, K., Kumutha, R., & Vishnuram, B. G. (2011). *Experimental investigations on mechanical properties of geopolymer concrete composites.*
- Vora, P. R., & Dave, U. V. (2013). Parametric studies on compressive strength of geopolymer concrete. *Procedia Engineering, 51*, 210–219.

## Reference

---

- Wallah, S. E. (2009). Drying shrinkage of heat-cured fly ash-based geopolymer concrete. *Modern Applied Science*, 3(12), 14–21.
- Weil, M., Dombrowski, K., & Buchwald, A. (2009). Life-cycle analysis of geopolymers. In *Geopolymers* (pp. 194–210). Elsevier.
- Xu, J. Z., Zhou, Y. L., Chang, Q., & Qu, H. Q. (2006). Study on the factors of affecting the immobilization of heavy metals in fly ash-based geopolymers. *Materials Letters*, 60(6), 820–822.
- Yu, Q. L. (2019). Application of nanomaterials in alkali-activated materials. In *Nanotechnology in Eco-efficient Construction* (pp. 97–121). Elsevier.
- Yunsheng, Z., Wei, S., Qianli, C., & Lin, C. (2007). Synthesis and heavy metal immobilization behaviors of slag based geopolymer. *Journal of Hazardous Materials*, 143(1–2), 206–213.  
<https://doi.org/10.1016/j.jhazmat.2006.09.033>
- Zhang, J., Provis, J. L., Feng, D., & van Deventer, J. S. J. (2008). Geopolymers for immobilization of Cr<sup>6+</sup>, Cd<sup>2+</sup>, and Pb<sup>2+</sup>. *Journal of Hazardous Materials*, 157(2–3), 587–598.
- Zhang, P., Zheng, Y., Wang, K., & Zhang, J. (2018). A review on properties of fresh and hardened geopolymer mortar. *Composites Part B: Engineering*, 152, 79–95.  
<https://doi.org/10.1016/j.compositesb.2018.06.031>
- Zhao, R., & Sanjayan, J. G. (2011). Geopolymer and Portland cement concretes in simulated fire. *Magazine of Concrete Research*, 63(3), 163–173.

## الخلاصة

تم اقتراح وتطوير نموذج رياضي جديد للتنبؤ بالخصائص الهندسية للخرسانة الجيوبوليمر المتضمنة مع مواد مضافات معدنية باستخدام معادلة الانحدار الخطي وهي شبكة عصبية اصطناعية (ANN). كان خلط العناصر المتناسبة مثل {الأسمنت ، والركام الناعم ، والركام الخشن ، والماء إلى المادة الرابطة ، والمضافات المعدنية مثل (الرماد المتطاير ، ودخان السيليكا ، والميتاكرولين ، وخبث الفرن العالي الحبيبي ، ورماد قشر الأرز)} هي المتغيرات المستخدمة في نماذج التنبؤ. تم أخذ التباين كمعاملات ناتجة لقابلية التشغيل والخصائص المتصلبة للخرسانة الجيوبوليمرية. ثم تتم مقارنة النتائج التي تم الحصول عليها باستخدام الطريقتين ومناقشتها. توفر النماذج تقديراً معقولاً لخصائص قوة الخرسانة الجيوسياسية التي تشتمل على مواد مضافات معدنية وقدمت ارتباطات جيدة مع البيانات المستخدمة في هذا البحث ، وفقاً للمراجعة.

كانت معاملات الارتباط للخرسانة الطازجة متضمنة النتائج المتوقعة (الركود) 0.8778 باستخدام برنامج SPSS. أثناء استخدام برنامج ANN يعطي 0.92 كمعامل ارتباط لنتائج الركود. كانت معاملات الارتباط للخرسانة الصلبة متضمنة مقاومة الانضغاط المتوقعة لمدة 3 و 7 و 28 و 90 يوماً 0.94 و 0.93 و 0.91 و 0.96 على التوالي. وكان معامل الارتباط للتنبؤ مقاومة الشد الانشقاقي 3 و 7 و 28 و 90 يوم 0.9333 و 0.95 و 0.903 و 0.94 على التوالي. تم قياس معاملات الارتباط لقوة الانحناء المتوقعة لمدة 3 و 7 و 28 يوماً 0.86 و 0.87 و 0.87 على التوالي. بالنسبة لمئات الخرسانة الجيوبوليمرية ، تم جمع نفاذية عند (90 يوم معالجة) للتنبؤ بمعاملات الارتباط ، والتي تساوي 0.97.

علاوة على ذلك ، على الرغم من الاختلافات في النتائج ، أظهرت النماذج المقدمة أنها أداة مفيدة في التنبؤ بقوة الضغط لمختلف أنواع الخرسانة الجيولوجية. تفوقت تلك التي تعتمد على الشبكات العصبية الاصطناعية على النماذج القائمة على نموذج الانحدار الخطي. إن استخدام الشبكات العصبية المصطنعة للتنبؤ بنقاط القوة الانضغاطية في الخرسانة المضافة في فترات معالجة مختلفة لها قدر كبير من الإمكانيات في جوانب المعادلات غير الخطية ، وهي جيدة بشكل خاص في تحديد الاتجاهات غير الخطية والعلاقات التي يصعب حسابها باستخدام التقنيات التقليدية.



جمهورية العراق

وزارة التعليم العالي والبحث العلمي

جامعة بابل كلية الهندسة

قسم الهندسة المدنية

# استخدام النمذجة للتنبؤ بالخصائص الهندسية لمونة الجيوبوليمر و الخرسانة التي تحتوي على المواد المضافة المعدنية

رسالة

مقدمة الى كلية الهندسة - جامعة بابل وهي جزء من متطلبات نيل درجة الدبلوم في  
الهندسة/ الهندسة المدنية

من قبل

تماره سباهي محسن رضا

(بكالوريوس)

بإشرافه

الأستاذ الدكتور حيدر محمد عويد